https://doi.org/10.5194/hess-2024-67
Preprint. Discussion started: 2 April 2024

Hydrology and Earth System Sciences
Discussions

Changes in flowing drainage network and stream chemistry during rainfall events for two pre-Alpine catchments

Izabela Bujak-Ozga[1,2], Jana von Freyberg[1,2], Margaret Zimmer[3], Andrea Rinaldo[1,4], Paolo Benettin[1,5], and Ilja van Meerveld[6]

[1]EPF Lausanne, School of Architecture, Civil and Environmental Engineering, Lausanne, Switzerland
[2]Swiss Federal Institute for Forest, Snow and Landscape Research (WSL), Mountain Hydrology and Mass Movements, Birmensdorf, Switzerland
[3]U.S. Geological Survey, Upper Midwest Water Science Center, Madison, Wisconsin, USA
[4]Università di Padova, Department of Civil, Environmental and Architectural Engineering (DICEA), Padova, Italy
[5]University of Lausanne, Department of Earth Surface Dynamics, Lausanne, Switzerland
[6]University of Zurich, Department of Geography, Zurich, Switzerland

Correspondence to: Izabela Bujak-Ozga (hydrology@izabelabujak.com)

Abstract. Many headwater catchments embed non-perennial streams that flow only during wet conditions or in response to rainfall events. The onset and cessation of flow results in a dynamic stream network that periodically expands and contracts. The onset of flow can flush sediment and nutrients from previously dry streambeds and enhance carbon processing rates. The expansion of the flowing drainage network also increases hydrologic connectivity between hillslopes and streams because it decreases travel distances to the stream. However, datasets on flowing drainage network dynamics during rainfall events and short-term changes in stream chemistry are rare. This limits our interpretation of hydrological processes and changes in stream chemistry during events.

Here, we present joint hourly measurements of solute concentrations and stable isotopes from precipitation and streamflow at the outlets of two 5-ha catchments in the Swiss pre-Alps during seven rainfall-runoff events in the snow-free season of 2021. Relevant samples were also collected from soil- and groundwater across the catchments before and after rainfall events. In addition, 10-min frequency information was collected on the flowing drainage network length. We used these synoptic measurements to infer the dominant runoff-generating mechanisms for the two experimental catchments.

Despite their proximity and similar size, soil and bedrock features, the flowing drainage network dynamics proved very different for the two catchments. In the flatter catchment (average slope: 15°), the stream network was more dynamic and expanded rapidly, up to 10-fold, while in the steeper catchment (average slope: 24°), it remained relatively stable (only a 2-fold change). The event water contributions were also higher for the flatter catchment. The dilution of calcium at the time of the rapid expansion of the network and increase in discharge suggested that the contribution of rainfall falling directly on the stream channels is important, especially for the smaller events during dry conditions. In wet conditions, unchanneled areas must have contributed event water as well. In the flatter catchment endowed with the more dynamic stream network, a "first

https://doi.org/10.5194/hess-2024-67
Preprint. Discussion started: 2 April 2024


Hydrology and Earth System Sciences
Discussions

flush" of nitrate was detectable, possibly attributed to the transport of material from previously dry stream segments. In the catchment characterized by a more stable flowing drainage network, such flush was not observed and nitrate concentrations decreased, suggesting enhanced contributions from riparian groundwater with reducing conditions during rainfall events. Our experimental study not only highlights the large differences observable in stream network dynamics and stream chemical responses for neighboring, nearly equal-size catchments but also shows the value of fine-scale observations on both the channel network dynamics and stream chemistry to fully understand runoff generation mechanisms.

1 Introduction

More than half of the stream network globally consists of streams that cease to flow for a certain time of the year (Messager et al., 2021) and this portion is expected to increase because of human-induced changes and climate change (Jaeger et al., 2014; Ward et al., 2020). The intermittent (i.e., non-perennial) stream network is a very dynamic system (Gregory and Walling, 1968) that often hosts high biodiversity and serves as a habitat to endemic species (Meyer et al., 2007; Acuña et al., 2014; Doods, 2004; Stubbington et al., 2017). Intermittent streams are also connectivity corridors (Rinaldo et al., 2018) that have important implications in metapopulation (Mari et al., 2014; Giezendanner et al., 2021) and ecosystem dynamics (Datry et al., 2023). However, major challenges persist in our understanding of how, when, and where flow in intermittent streams occurs (Fovet et al., 2021). Specifically, the link between the runoff-generation mechanism, stream network expansion and contraction and biogeochemical processes has not yet widely been investigated (Covino, 2017; Zimmer et al., 2022).

The effects of flow intermittence and related drying and re-wetting cycles on nutrient cycling have been studied for stream reaches (Datry et al., 2023). The onset of flow can lead to the flushing of sediment (von Schiller et al., 2017) and the mobilization of coarse particulate organic matter (Lamberti et al., 2017) that were stored in the dry streambed. Temporarily connected streams can be significant sources of carbon (Thoms 2003; Thoms et al. 2005), organic matter and nutrients (Shumilova et al., 2019) to downstream rivers. The onset of flow in previously dry streambeds also increases biogeochemical processing rates (von Schiller et al., 2017, Burrows et al. 2017; Addy et al., 2019). The CO_2 efflux from dry streambeds can be substantial (Keller et al., 2020) also compared to that from surrounding soils (Arce et al., 2019) and higher than from channels with flowing or standing water (von Schiller et al., 2014).

The dynamic variations in wetness and flow conditions along drainage networks influence the quantity and quality of streamwater at the catchment outlet. In addition, to the changes in stream chemistry due to in-channel processes, stream chemistry is also affected by changes in the relative contributions of different flow pathways (Knapp et al., 2022). When the flowing drainage network expands, the hydrologic connectivity between hillslopes and the streams increases and flow pathways become shorter (van Meerveld et al., 2019). Water in intermittent streams may have a different chemical composition from that in perennial streams, e.g., because it contains less deep groundwater and is primarily fed by near-surface flow

https://doi.org/10.5194/hess-2024-67
Preprint. Discussion started: 2 April 2024


Hydrology and Earth System Sciences
Discussions

pathways. Warix et al. (2022) used CFC-11 and CFC-12 measurements in intermittent streams and showed that deep flowpaths contributed to all streams, but that cessation of near-surface flowpaths was responsible for stream drying. Zimmer and McGlynn (2018) combined measurements of the wet portion of the drainage network with measurements of DOC concentrations in two 3.3 and 48.4 ha catchments in North Carolina, USA. They found that DOC export and streamflow dynamics were driven by the connection and disconnection of lateral, longitudinal, and vertical source areas and associated changes in dominant flow pathways. Hale and Godsey (2019) showed that seasonal-scale DOC dynamics were strongly related to indices describing streamflow intermittency and that DOC concentrations were more stable in locations where the flow was more persistent. These studies demonstrate that flowing drainage network dynamics are closely linked to the variations in streamwater chemistry, but the relation is not yet well established.

This lack of understanding of how the changes in flowing drainage network lengths affect solute concentration dynamics is caused by technical challenges in measuring both variables. Field surveys are used to determine the seasonal flowing/wet portions of the drainage network (e.g., Godsey and Kirchner, 2014; Botter and Durighetto, 2020; Durighetto et al., 2020; Warix et al., 2021) and its dynamics during rainfall events (Durighetto and Botter, 2021; Bujak-Ozga et al., 2023), but are time-consuming. Water presence sensors (Jaeger et al., 2012; Jensen et al., 2019; Kaplan et al., 2019; Zanetti et al., 2022) and multi-sensor monitoring systems (Assendelft and van Meerveld, 2019) are useful for determining the wet and flowing portion of the drainage network, respectively, but the number of locations that can be easily maintained is limited due to the time required for maintenance, especially in mountainous catchments where streambeds are unstable. Still, the number of available datasets from research catchments is increasing. Recent research efforts have focused on describing the general patterns of the dynamics of drainage networks (Botter et al., 2021; Price et al., 2021; Durighetto and Botter, 2022), use of probabilistic (Durighetto et al., 2022) and machine-learning (Mimeau et al., 2024) methods to predict drainage network dynamics based on limited field data, and, finally, physically based models (Ward et al., 2018). Thus, high temporal resolution information on the dynamics of stream networks is now becoming available.

Considering the potential importance of intermittent stream dynamics to affect stream chemical responses during rainfall events, and the lack of high-resolution data for both the drainage network and solute concentrations, we investigated the dynamic changes in flowing drainage networks and streamwater chemistry in two Swiss pre-Alpine catchments. Specifically, we address the following research questions:

(1) How do solute concentrations and flowing drainage networks change during rainfall events, and how are these dynamics related to event characteristics?

(2) How do solute concentrations and flowing drainage network dynamics differ for two catchments with different lengths of geomorphic channel networks?

(3) What runoff-generation mechanisms are consistent with the observed solute concentrations and flowing drainage network dynamics?

https://doi.org/10.5194/hess-2024-67
Preprint. Discussion started: 2 April 2024


Hydrology and Earth System Sciences
Discussions

100 The joint measurements of the flowing drainage network and solute concentrations were taken during rainfall events in the snow-free season of 2021. The neighboring catchments have similar sizes, soils, and geology but differ in topography and the length of the channel network.

2 Methodology

2.1. Study sites

105 #### 2.1.1 Location and topography

This study was carried out between June and October 2021 in two tributaries of the Erlenbach (Erl; 0.7 km2) research catchment in the Swiss pre-Alps (Stähli et al., 2021), located approximately 40 km southeast of Zurich (Fig. 1). The two studied tributaries are referred to as Lan and Cha, based on the local names of the areas that they drain (Langried and Chasperböden, respectively). The 0.048 km^2 Lan catchment ranges from 1195 to 1292 m a.s.l. in elevation. With an average slope of 15°, Lan
110 represents the flatter and lower part of the Erl catchment. The geomorphic channel network extends over most of the Lan catchment (Fig. 1). The Cha catchment has a similar size as Lan (0.048 km^2), but it is located at a higher elevation (1487 to 1656 m a.s.l) in the steeper (average slope 24°) part of the Erl catchment. The upper half of the Cha catchment is particularly steep, likely due to a fault zone between two types of Flysch bedrock (Fig.1; Bujak-Ozga et al., 2023). In Cha, springs emerge near the bottom of the steepest slope and stream channels are located only in the lower, flatter portion of the catchment.

115

https://doi.org/10.5194/hess-2024-67
Preprint. Discussion started: 2 April 2024

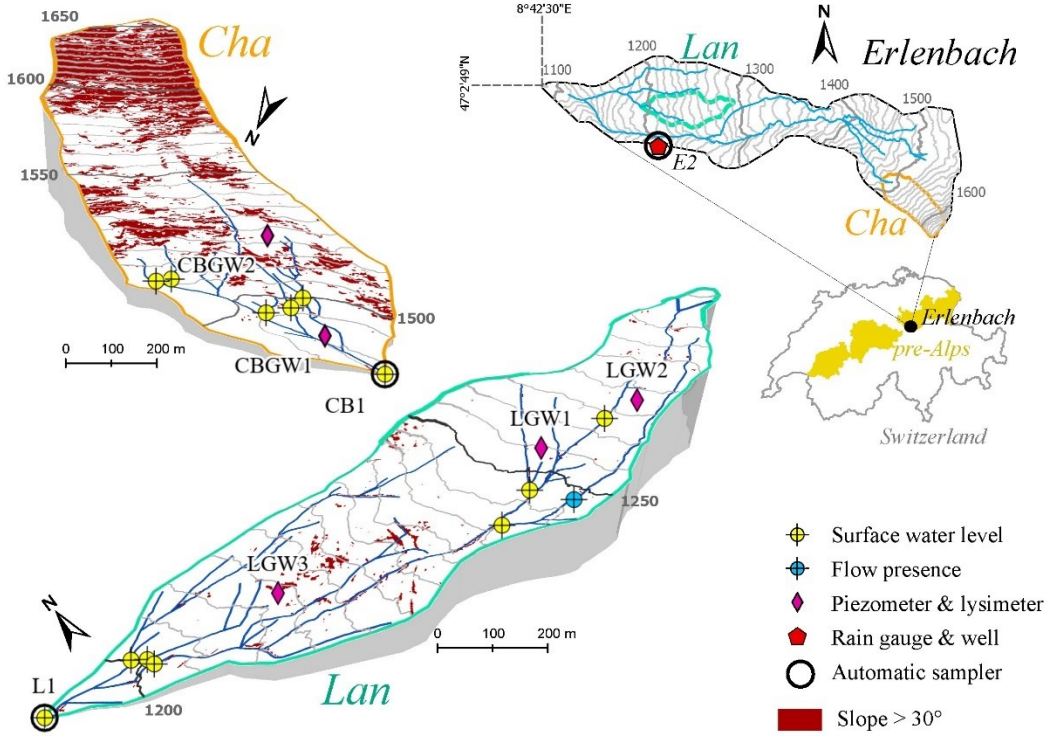

Figure 1: Maps on the left show the two study catchments Langried (Lan; blue) and Chaspersböden (Cha; orange) and the monitoring network in each catchment. The maps on the right show the location of Cha and Lan in the Erlenbach (Erl) catchment (upper) and the location of the Erl catchment and the pre-Alps in Switzerland (lower). The grey lines represent the 5 m contour in Lan and Cha and the 10 m contour lines in Erl and are based on the digital elevation model with a 0.5 m resolution (SwissALTI3D, SwissTopo). The dark red shading represents areas with slopes >30°. The coordinate system is CH1903/LV03.

2.1.2 Climate

The average annual precipitation at 1210 m a.s.l. in the Erl catchment is 2266 mm (water years 1969–2019; Stähli et al. 2021), of which approximately one-third is snow. Although an up to 2 m thick continuous snow cover can be present from December to April, at lower elevations it is often interrupted by winter rainfall (von Freyberg et al. 2022). The mean monthly temperature ranges from -1.9 °C to 15.9 °C (von Freyberg et al. 2022). On average, it rains every second day in summer (van Meerveld et al., 2018) but the summer of 2021, and especially July 2021, were very wet. Total precipitation between June 1st and October 1st was 1154 mm, compared to an average between 2010 and 2020 of 954 mm (range: 609-1395 mm; Stähli, 2018). Total precipitation in July 2021 was 548 mm, almost three times the average of 190 mm and higher than measured between 2010 and 2020 (range: 7-530 mm; Stähli, 2018).

https://doi.org/10.5194/hess-2024-67
Preprint. Discussion started: 2 April 2024


Hydrology and Earth System Sciences
Discussions

2.1.3 Geology, pedology, and land-use

The geology of the Erlenbach catchment is flysch (Hantke et al., 2022). The flysch bedrock is overlain by 1-2 meter thick clay-rich gleysols. Because the gleysols are locally quite shallow and have a very low permeability, groundwater levels remain close to the surface in a large part of the catchment, especially in the flatter areas (Rinderer et al., 2014). Holocene deposits interspersed by Pleistocene moraine (till) deposits can be found in the Lan catchment and the lower part of the Cha catchment (Hantke et al., 2022).

The Lan catchment is partly covered by forests, grasslands, and wet meadows. The coniferous forest is dominated by Norway spruce (*Picea abies*) and silver fir (*Abies alba*) (Stähli et al., 2021). In contrast, the Cha catchment is mainly covered by grassland and wet meadows, especially in the western part. There are a few isolated groups of trees, including Norway spruce (Picea abies) and silver fir (Abies alba), mainly in the eastern part of Cha (Stähli et al., 2021). The Cha catchment is used as pasture for cattle during summer.

2.2. Hydrometric measurements and data

Stream water levels were monitored every 5 min with air pressure and temperature-compensated pressure transducers (CTD10, Meta, Pullman, Washington, USA) and pressure transmitters (26Y, Keller AG, Winterthur, Switzerland) at ten locations in Lan and eight locations in Cha (Fig. 1). At the catchment outlets, stream water levels were measured behind a V-notch weir. These measurements were converted to discharge time series using the Kindsvater-Shen equation (Kulin and Compton, 1975). At all other locations, the pressure transmitters were placed directly in the middle of the channel cross-section.

For groundwater monitoring, piezometers were installed at three locations in Lan (LGW1-LGW3) and two locations in Cha (CBGW1, CBGW2). The piezometers were 1.19-1.44 m deep and screened over the lowest 50 cm. Groundwater levels were monitored every 5 min using pressure transducer (LGW1) and transmitters (LGW2-3). For Lan, data are available from the 1st of June to the 27th of October 2021 for all measurement locations, except for LGW3 for which data are available from the 9th of September 2021 onwards. For Cha, data are available from the 18th of June to the 27th of October 2021 for all measurement locations, except for the outlet (CB1) for which data are available from the 1st of June 2021. Data gaps of up to a few hours occurred sporadically due to data transmission errors and measurement disturbances (e.g., during sensor maintenance or water sample collection).

Precipitation data at 1210 m a.s.l. at the Erlenhöhe climate station near Lan (E2; Fig. 1) were provided by the WSL's Mountain Hydrology and Mass Movements research unit. These data are available at a 10 min resolution and were measured using a tipping bucket rain gauge (Pluvio2 L400 RH, Ott Hydromet GmbH, Switzerland).

https://doi.org/10.5194/hess-2024-67
Preprint. Discussion started: 2 April 2024


Hydrology and Earth System Sciences
Discussions

2.3. Channel flow state surveys

On the 2nd and 4th of June 2021, we mapped the complete geomorphic channel network in both catchments. We defined a channel as a depression or landscape feature where directed surface flow occurs or where there are visible signs that flow occurred in the recent past (i.e., in the last few months). The entire channel network was divided into 85 and 48 reaches with a median length of 18 m and 13 m in Lan and Cha, respectively (cf. supplementary information to Bujak-Ozga et al. 2023). The start and end of the reaches were defined based on similar hydrologic conditions along each reach (i.e., expected drying and rewetting patterns based on locally observed water level, wetness, slope, channel width, and streambed material; Fig.S1).

We carried out eighteen spatial streamflow presence or absence mapping surveys in Lan and fifteen surveys in Cha. During each mapping survey, we classified all reaches as either "flowing" or "not flowing". These surveys took up to approximately 5 hours in Lan and 3 hours in Cha. To better delineate the flow regime within the catchment and help achieve higher reproducibility, we further categorized "flowing" reaches as weakly trickling (<1.0 [l min^{-1}]), tricking (2.0-1.0 [l min^{-1}]), weakly flowing (5.0–2.1 [l min^{-1}]), or flowing (>5.0 [l min^{-1}]) based on a visual estimate of the flow and bucket measurements when the visual classification was difficult. The "not flowing" reaches were further categorized into either standing water, wet streambed, or dry streambed. Besides the regular catchment-wide mapping surveys, we reported our visual observations of the channel flow state for selected reaches during equipment maintenance. We gathered the georeferenced measurements of the channel flow state, water levels, photos and videos using the TempAqua App iOS (Bujak-Ozga, 2023). At one location (marked with blue in Fig. 1) mapping surveys were complemented by continuous flow presence measurements with a multi-sensor monitoring system (Assendelft and van Meerveld, 2019). Because the flow needs to be higher than 1.0 [l min^{-1}] for the flow sensor (propeller) to register flow, we only used the data when the sensor recorded flowing water. We did not use the sensor measurements when it registered the not-flowing state because the flow in the channel could be between 0 and 1.0 [l min^{-1}].

2.4. Hydrochemical data

2.4.1 Sample collection

Between the 5th of August and the 22nd of October 2021, we collected water samples from streams, soil, and groundwater in the Lan and Cha catchments and from rainfall. Stream water samples were collected at the outlets of the Lan and Cha catchments shortly before and hourly during seven and six rainfall events, respectively, using MAXX autosamplers (P6, MAXX GmbH, Germany). Rainwater samples were collected hourly during the same events at location E2 (Fig.1) using a MAXX autosampler as well (P6, MAXX GmbH, Germany). In addition, we conducted a spatial sampling campaign during dry (baseflow) conditions on the 7th of September 2021. Grab samples were collected at the beginning of every channel reach that had standing or flowing water (thirty samples in Cha and nine in Lan).

https://doi.org/10.5194/hess-2024-67
Preprint. Discussion started: 2 April 2024


Hydrology and Earth System Sciences
Discussions

Groundwater samples and soil water samples were collected before and after rainfall events and during the spatial sampling campaign. Soil water samples were collected using suction lysimeters installed at a depth of 30-35 cm, i.e., at the boundary between the rooting zone and the denser clay of the gleysols. The applied pressure was ~60kPa. Groundwater samples were collected from the piezometers. The longest period without groundwater and lysimeter sample collection was nine days (between the 18th and 27th of August). In total, we collected 149 and 136 streamflow samples at the outlet during events, 98 and 118 streamflow samples at the outlet during baseflow, 68 rainfall samples, 55 and 37 soil water samples, and 37 and 29 groundwater samples for the Lan and Cha catchments, respectively.

2.4.2. Laboratory analysis

All water samples were filtered using 0.45 µm Teflon membrane filters and stored refrigerated before analysis at the WSL central laboratory in Birmensdorf, Switzerland. The samples were analyzed for major anions using ion chromatography (Integrion HPIC, Dionex Corporation, USA). For the analysis of major cations, the samples were acidified (HNO_3) and subsequently analyzed using optical emission spectrometry with inductively coupled plasma (ICP-OES Optima 7300, PerkinElmer, Inc., USA). The samples were analyzed for the stable isotopes of hydrogen and oxygen of the water molecule using laser isotope spectrometry (IWA-45-ER, Los Gatos Research, ABB Ltd., Switzerland). The stable isotope values are reported relative to the V-SMOW2 standard using the delta (δ^2H and $\delta^{18}O$) notation. The measurement accuracy is ±1.0‰ and ±0.5‰ for δ^2H and $\delta^{18}O$, respectively, while the measurement precision is ±2‰ and ±1‰ for δ^2H and $\delta^{18}O$, respectively.

2.5. Data analyses

2.5.1 Rainfall events

We classified the precipitation and discharge time series into rainfall-runoff events. We define the start of a rainfall-runoff event as the onset of precipitation resulting in a substantial increase (>150%) in discharge at the Lan outlet. The end of an event either marks the time when discharge returned to the pre-event level or the start of the following event. Based on this definition of events, there were twelve events in both catchments. Hydrochemical data were collected for seven and six of them in Lan and Cha, respectively. The event starts and ends are the same for both catchments since the samples were collected only at an hourly resolution and the time difference in the streamflow response was minimal due to the proximity of the two catchments.

We also evaluated the antecedent wetness conditions for the twelve events based on the average discharge during the 48 hours before the event (Q_{48}). We chose Q_{48} because it reflected the groundwater level measured in the Erl catchment (E2) well. Q_{48} was < 4.5 [l min^{-1}] when the groundwater levels had dropped to a relatively stable level of 142 cm below the surface at location

https://doi.org/10.5194/hess-2024-67
Preprint. Discussion started: 2 April 2024


Hydrology and Earth System Sciences
Discussions

E2, we use this threshold to divide the events into those that had dry antecedent conditions, and those with wet antecedent conditions (cf. Bujak-Ozga et al., 2023). As a second indicator of the antecedent wetness conditions, we calculated the cumulative precipitation during the 48 hours before the start of the event (P_{48}; cf. Kiewiet et al., 2019). Q_{48} and P_{48} were correlated (Spearman rank correlation rs: 0.44, p=0.023) and therefore, we mainly report Q_{48} in the text.

2.5.2 Flowing drainage network and flow persistency

We obtained time series of the flowing drainage network lengths (FDNL) and spatial maps of the flow/no-flow conditions at a 10-min resolution using the CEASE method (Bujak-Ozga et al., 2023). In short, this method combines the data from the mapping surveys with the data from the water level sensors to obtain time series of "flow" and "no flow" for each reach. The water level at the times of the surveys is used to determine for each reach the threshold water level above which the stream reach was flowing. This threshold is then used to obtain a time series of "flow" and "no flow" for the reach. This is done for each reach, for each of the water level sensors. The time series of "flow" and "no flow" for each reach (based on the different water level sensors) are compared and a final decision on "flow" and "no flow" for each time step is based on the majority vote. This leads to a continuous time series of "flow" and "no flow" for each stream reach. By summing up the length of all flowing reaches for each time step, we obtain the FDNL for the entire catchment. Because the FDNL differs for both the Lan and Cha catchments, we normalized the FDNL values by dividing them by their maxima. Thus, fFDNL is the fraction of the total drainage network that (according to the CEASE method) had flowing water. Finally, for each channel reach we calculated the fraction of time it was flowing, which we refer to as the local flow persistency. Here a value of 1 indicates that according to the CEASE method the reach was always flowing and a value of 0 indicates that the reach was never flowing. Detailed analyses by Bujak-Ozga et al. (2023) showed that the method selected the right flow state for >94% of the time that visual observations of flow or no flow conditions were available.

2.5.3 Characterisation of groundwater chemistry

The hydrochemical composition of groundwater can be spatially very heterogeneous, as shown for the neighboring Studibach catchment by Kiewiet et al. (2019). To characterize the hydrochemical composition of groundwater, we used three different sets of water samples collected during baseflow conditions: (1) groundwater samples, (2) streamwater samples from the catchment outlets and (3) streamwater samples collected during the snapshot campaign. Here, we assume that streamwater samples collected during baseflow conditions reflect the average hydrochemical composition of the groundwater that contributes to streamflow. The results from the snapshot campaign and the groundwater samples are useful to assess the spatial variability of the shallow groundwater before it reaches the catchment outlet.

https://doi.org/10.5194/hess-2024-67
Preprint. Discussion started: 2 April 2024


Hydrology and Earth System Sciences
Discussions

2.5.4 Hydrograph separation and end-member mixing analysis

We calculated the event-water fractions (f_e) for the streamwater samples using the isotope data in a two-component hydrograph separation, following the procedure described in von Freyberg et al. (2018). We use these event water fractions as a proxy for rain falling on the stream channels and saturated areas (direct rainfall runoff) or very fast flow of event water through the topsoil (depth 0-15 cm). For four events, isotope-based hydrograph separation was not possible because the δ^2H values for streamflow and precipitation partly overlapped (Fig.S3, Fig.S5 - S7, Table 1). We estimated the uncertainties in f_e using the Gaussian error-propagation method (Genereux, 1998). The oxygen and hydrogen isotopes data yielded similar results, thus, we report only the results based on hydrogen stable isotopes due to their better precision to measurement range ratio.

The calculated event water fractions were used together with the concentrations in rainfall and the pre-event water to determine the "expected streamwater concentration" based on mixing of rainfall and pre-event water (i.e., the concentration that should be expected if streamflow consisted only of a mixture of pre-event water and event water). Deviations from this expected concentration are either due to the contributions of different sources or biogeochemical reactions.

Furthermore, we evaluated the flow contributions from the subsoil (depth of approximately 30 cm; f_{sw}) based on the End Member Mixing Analysis (EMMA; Christophersen and Hooper, 1992) using the silica concentrations and hydrogen isotope data from the soil water, rainfall and baseflow (outlet) samples.

3 Results and discussion

3.1 Chemical composition of the different water sources

3.1.1 Rainfall

Solute concentrations in rainfall were very low and close to the detection limits for all measured indicators except nitrate and sulfate whose median concentrations were 0.6 and 0.3 [mg l^{-1}], respectively (Fig. 3). The stable isotope composition in rainfall varied widely (median = -72.8‰ and IQR = 52.8‰ for δ^2H; Fig. 2), especially between rainfall events (Fig. 4b, Fig. S4b-S8b).

https://doi.org/10.5194/hess-2024-67
Preprint. Discussion started: 2 April 2024

Hydrology and Earth System Sciences
Discussions

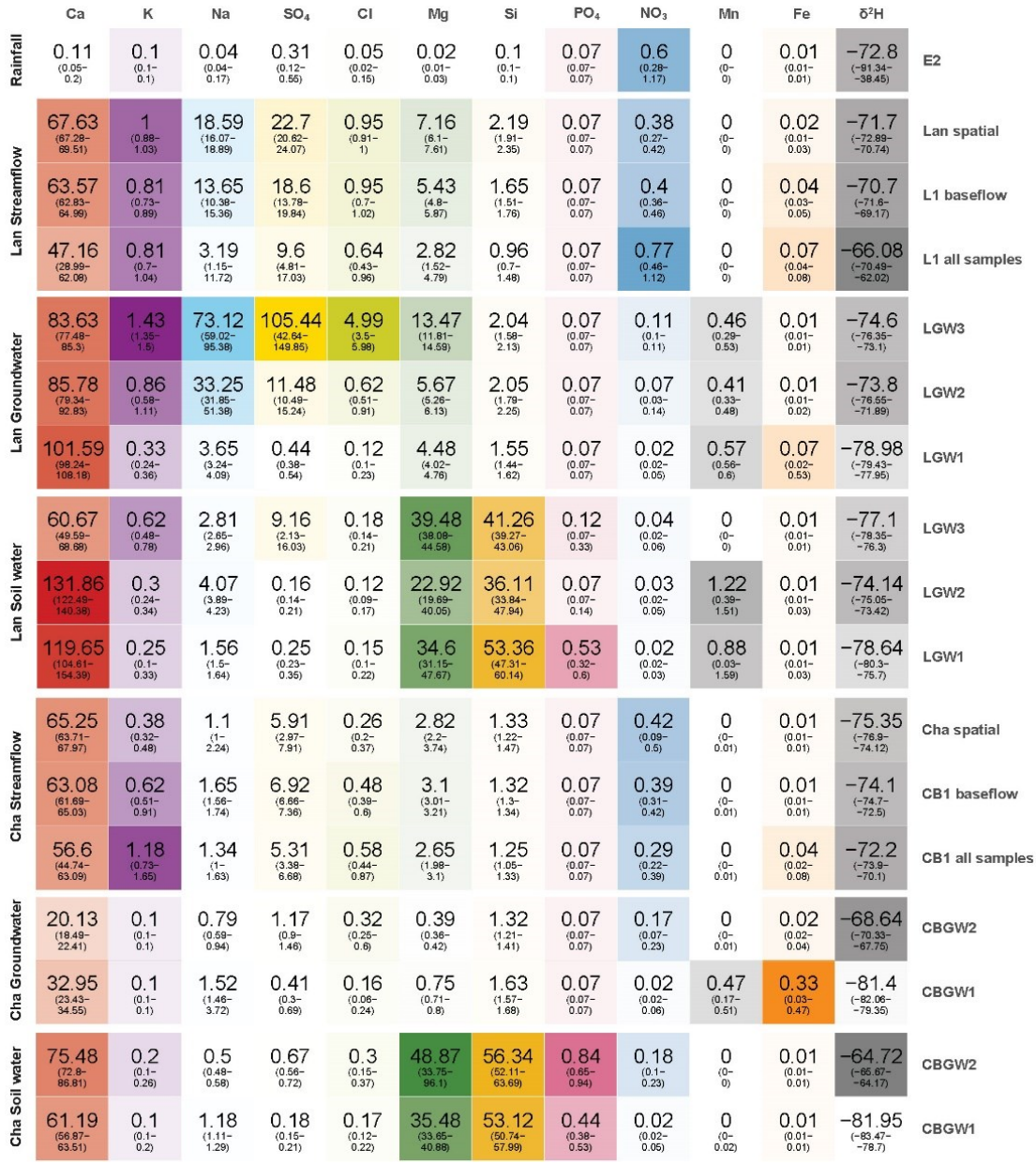

Figure 2: Median solute concentrations (and interquartile range IQR in parentheses) for all measured solutes and locations sampled in the Lan and Cha catchments during the entire monitoring period (both for baseflow conditions and rainfall events). All solute concentrations are in [mg l^{-1}]. Note that the intensity of each color reflects the median solute concentration. Location names are shown on the right (see Figure 1). The terms "Cha spatial" and "Lan spatial" refer to the samples collected during the spatial sampling campaign in the Cha and Lan catchments, respectively.

https://doi.org/10.5194/hess-2024-67
Preprint. Discussion started: 2 April 2024


Hydrology and Earth System Sciences
Discussions

3.1.2. Groundwater

Comparison of the different datasets

Solute concentrations in Lan's groundwater were spatially heterogeneous. They differed among the three locations in Lan (Fig. 2): moving uphill from LGW1 to LGW3, calcium concentrations decreased, while potassium, sodium, sulfate, chloride, and magnesium concentrations increased. Walker et al. (2003) attributed a high spatial variability in the groundwater chemistry in headwater catchments to short flowpath lengths and limited internal mixing within a catchment. This supports a marked dependence on local conditions unbuffered by transport phenomena. On the contrary, the chemical composition of groundwater was similar for the two monitoring locations in Cha (Fig. 2; Fig. S1-S2).

The groundwater concentrations in the Lan catchment were similar to those collected in baseflow at the outlet, except for calcium and manganese (higher in groundwater), and nitrate, iron, and sulfate (lower in groundwater) (Fig. 3). In the Cha catchment, groundwater differed from baseflow at the outlet for most solutes (Fig. 3). For both catchments, there was no statistical difference between the streamwater baseflow samples taken at the outlet and those taken throughout the catchment, except for potassium in both catchments and chloride in Cha (Fig.S2), but even for these solutes, the differences in the concentrations were very small (e.g. around 0.2 [mg l^{-1}] for potassium). The similarity of the two types of baseflow samples suggests that the samples collected at the outlets are representative for the integrated groundwater signal.

Description of baseflow chemistry

Baseflow was in both catchments characterized by high concentrations of weathering-derived solutes. Calcium and sulfate were the most abundant solutes in both catchments. Calcium concentrations are high due to the weathering of the limestone and marl in the flysch bedrock. However, baseflow concentrations at the Lan outlet were lower and less variable than in the groundwater (as shown by other studies in this area, e.g., Fischer et al., 2015), suggesting that the oversaturated calcium in groundwater precipitates once it reaches the streams and physical conditions change. Furthermore, the groundwater concentrations were much higher and more spatially variable in Lan than in Cha groundwater (Fig. 3). The more acidic conditions in the forested Lan catchment could lead to a higher solubility and higher concentrations (Gal et al, 1996) in Lan than Cha. A high spatial variability in groundwater concentrations is not surprising as Kiewiet et al. (2020) showed for the neighboring Studibach catchment that calcium concentrations in shallow groundwater can vary by 22 [mg l^{-1}] (standard deviation). The calcium concentrations in baseflow at Cha were similar to those in Lan but higher than measured in the groundwater. This suggests that the piezometers in Cha may not be fully representative of all the groundwater that contributes to baseflow and that another, perhaps deeper, source of groundwater contributes to streamflow at the outlet of Cha. This would be consistent with the statistically significant difference between the concentrations in the groundwater and baseflow for the majority of other solutes as well (Fig. 3).

https://doi.org/10.5194/hess-2024-67
Preprint. Discussion started: 2 April 2024

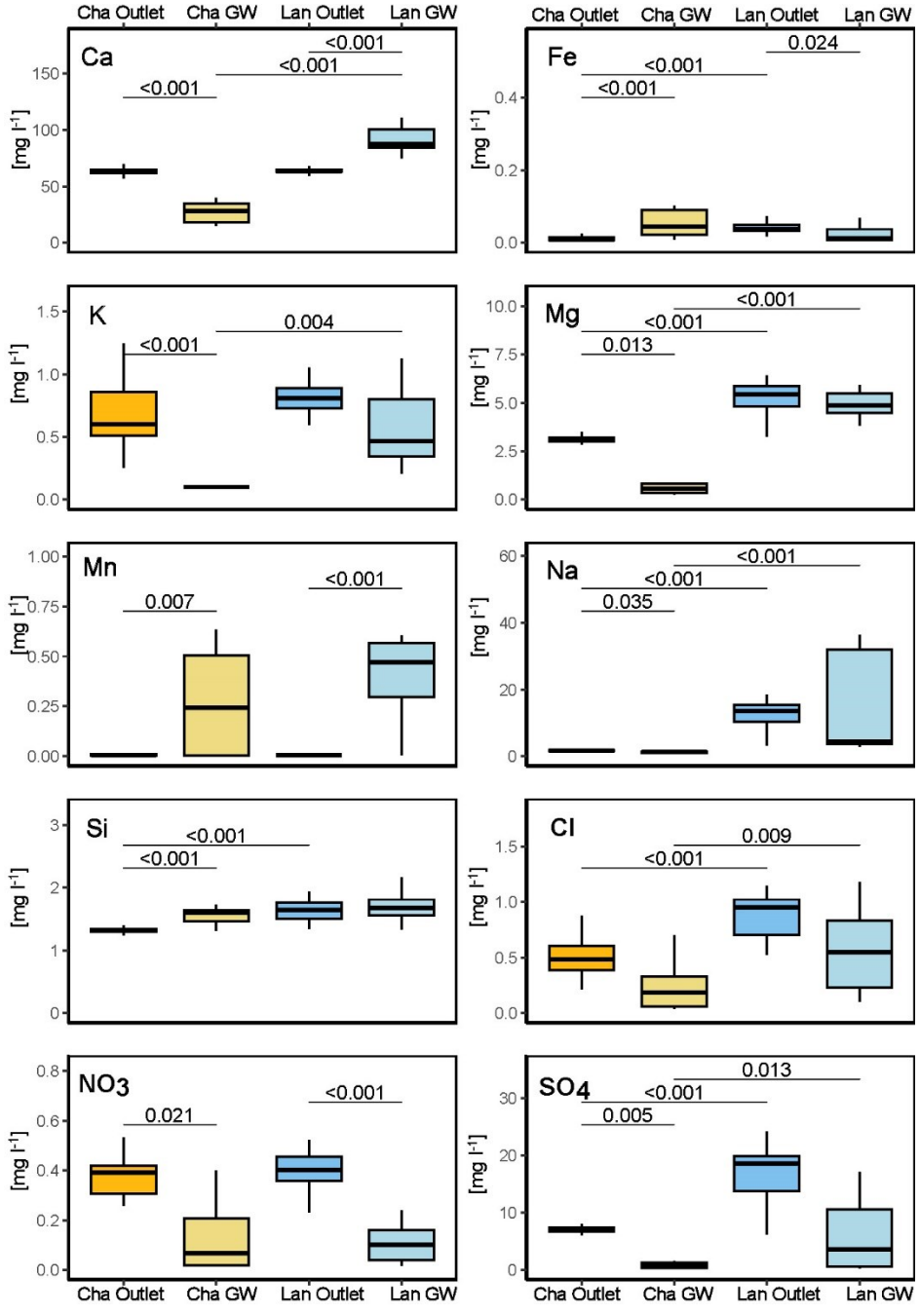

325 **Figure 3: Boxplots of the concentrations for selected solutes in baseflow at the catchment outlet (i.e., locations L1 and CB1) and groundwater (i.e., LGW1-LGW3, and CBGW1-2) in the Lan and Cha catchments. The boxes extend from the 1st to the 3rd quartile and the whiskers from the minimum to the maximum values. The lines represent the median values. The significance of the difference in the median solute concentrations was determined using the Kruskal-Wallis test with a Dunn post-hoc test. The thin horizontal lines above the boxes indicate significant differences ($p<0.05$) between the concentrations in baseflow and groundwater (intra-**
330 **catchment comparison) or between the two catchments (inter-catchment comparisons).**

https://doi.org/10.5194/hess-2024-67
Preprint. Discussion started: 2 April 2024


Hydrology and Earth System Sciences
Discussions

Sulfate and sulfur concentrations in Lan groundwater were spatially and temporarily variable and generally higher than in Cha groundwater and baseflow (Fig. 2-3). Fischer et al. (2015) suggested that in Erlenbach (Erl) and five neighboring catchments Anhydrite-rich groundwater from deep aquifers could contribute to streamflow. It is possible that the two wells (LGW3, LGW2) located closer to the main channel that cut into the flysch bedrock, received water from a deeper and Anhydrite-rich source. Kiewiet et al. (2019) suggested that high sulfate concentrations in groundwater in the neighboring Studibach catchment could be related to pyrite weathering. However, in Lan and Cha, the locations with high sulfate concentrations were partially different from those with high iron concentrations. Therefore, the contribution of a deeper Anhydrite-rich source of water in the Erlenbach catchment explains the variability in our data better than pyrite weathering.

Chloride concentrations in Lan groundwater were spatially and temporarily variable, but more stable (and lower) in Cha (Fig. 2 - 3). Chloride concentrations in baseflow (outlet) were much higher (with medians of 0.95 and 0.48 [mg L^{-1}] for Lan and Cha, respectively) than in rainfall (median = 0.05 [mg L^{-1}]), which is usually considered the main source of chloride in undisturbed catchments (e.g., Peck and Hurle, 1973; Neal and Kirchner, 2000). Knapp et. al (2020) found higher than expected concentrations of chloride in the Erlenbach during the growing season but, when they considered the whole hydrologic year, the chloride concentrations could be reasonably well explained by the precipitation inputs. Schleppi et al. (1998) also reported relatively high chloride concentrations in Erlenbach stream water in comparison to inputs measured as bulk deposition and suggested that dry deposition may contribute to the higher chloride output.

Nitrate concentrations were very low in groundwater (median concentrations < 0.1 [mg l^{-1}]), but significantly higher in baseflow for both catchments (Fig. 2). Slightly higher nitrate concentrations were only detected in one well, located on the Cha hillslope (median = 0.17 [mg l^{-1}] at location CBGW2; Fig. 3). Nitrate in the Erlenbach catchment originates from precipitation with minor inputs from grazing cattle in the upper catchment (Fig. 3; Knapp et. al, 2020).

3.1.3 Soil water

Soil water collected at a depth of ~30 cm was more enriched in silica, magnesium, phosphorus, and orthophosphate than groundwater (Fig. 3). Similar to the groundwater, soil water concentrations were higher in Lan than Cha (Fig. 2). The temporal variations in soil water concentrations at a sampling site were smaller than the differences between the sampling sites (Fig. 3). This high spatial variation compared to the temporal variation was also observed for the neighboring Studibach catchment (Kiewiet et al., 2019). High magnesium concentrations were found in soil water in the neighboring Studibach catchment as well (Kiewiet et al, 2020). The generally low concentrations of silica and magnesium in baseflow samples suggest that soil water does not contribute substantially to baseflow and that streams were mainly fed by groundwater (Fig. 2-3).

https://doi.org/10.5194/hess-2024-67
Preprint. Discussion started: 2 April 2024


Hydrology and Earth System Sciences
Discussions

In both catchments nitrate, sulfur, sulfate, sodium, potassium, iron, and chloride concentrations in soil water were relatively low compared to the groundwater (Fig. 2). Previous research in an area close to Lan showed that nitrate was present in low concentrations only in the topsoil (0-10 cm depth). In deeper layers, nitrate, and ammonia concentrations were negligible, and dissolved organic nitrogen was the predominant form of nitrogen (Hagedorn et al., 2001).

3.2. Changes in hydrochemistry and the flowing drainage network during events

3.2.1. Description of the events

The events on 2021-09-10, 2021-09-29, and 2021-10-21 were similar in size (total precipitation between 11 and 16 mm) and occurred during dry antecedent conditions (Table 1). However, the 2021-10-21 event was shorter than the other two events, resulting in a larger streamflow response and higher event water fractions compared to the other two small events. The events on 2021-10-12 (P = 23 mm) and 2021-08-28 (P = 28 mm) were moderate in size and occurred when antecedent conditions were wet. For Lan, this event resulted in a large streamflow increase (Table 1). This was not the case for Cha because part of the precipitation fell as snow. The 2021-09-19 and 2021-09-16 events were the largest and most intense events. The antecedent conditions were dry for the event on 2021-09-16, but wet for the event on 2021-09-19. Furthermore, the event on 2021-09-16 had a shorter duration and higher intensity leading to a very large increase in streamflow and expansion of the drainage network length (ΔQ = 1140 and 1634 [l min^{-1}] and ΔfFDNL= 0.78 and 0.36 for Lan and Cha, respectively; Table 1).

The isotope-based hydrograph separation for the events 2021-09-10, 2021-09-29, and 2021-10-21 yielded maximum event water fractions (f_e, max) between 0.20 and 0.48 for Lan and between 0.13 and 0.26 for Cha (no data for 2021-10-21; Table 1). The maximum event-water fractions were correlated with the changes in flowing network length (for Lan: r=0.99, p=0.019, n=3). Notably a one-fold change in f_{FDNL} was accompanied by a ~1.5-fold change in the maximum event-water fractions.

https://doi.org/10.5194/hess-2024-67
Preprint. Discussion started: 2 April 2024

Hydrology and Earth System Sciences
Discussions

Table 1: Overview of the seven events that were sampled for hydrochemical analysis. Events are ranked by the total event precipitation P [mm]; Q_{48} is the average streamflow in the two days before the event [l min^{-1}]; P_{48} is the total precipitation in the two days before the event start [mm]; GWL_{48} is the groundwater levels measured at location E2 (in cm below the surface), Q/P is the unitless runoff coefficient (event total streamflow per unit area divided by the total precipitation); ΔQ is the increase in streamflow during the rainfall-runoff event, i.e., the difference between streamflow at the time of the event start and the peak [l min^{-1}]; T_{peak} is the time between rainfall start and peak discharge (hours); Duration is the time (hours) between event start and end (see section 2.5.1); f_e, max the maximum event water fraction (± standard error) [-]; and Δf_{FDNL} is the change in the f_{FDNL}. The event on the 21st of October was sampled only in Lan.

Indices	Variable	Units	Site	Sep 10	Oct 21	Sept 29	Oct 12	Aug 28	Sep 19	Sep 16
Rainfall event	P	mm	Both	11	15	16	23	28	31	34
	Q/P	-	Lan	0.05	0.20	0.20	0.39	0.42	0.41	0.31
			Cha	0.50	0.35	0.50	0.34	0.7	0.45	0.38
	ΔQ	l·min^{-1}	Lan	16	370	116	529	707	686	1140
			Cha	408	891	219	57	648	833	1634
	T_{peak}	h	Lan	1	3	24	12	23	7	8
	Duration	h	Both	75	55	115	126	123	99	66
	$f_{e, max}$	-	Lan	0.20 ± 0.03	0.48 ± 0.05	0.34 ± 0.03	-	-	-	-
			Cha	0.26 ± 0.05	-	0.13 ± 0.03	-	-	-	-
	Δf_{FDNL}	-	Lan	0.32	0.70	0.52	0.61	0.58	0.51	0.78
			Cha	0.33	0.39	0.26	0.15	0.28	0.25	0.36
Antecedent wetness	P_{48}	mm	Both	2	0	0	0	3	0	4
	Q_{48}	l·min^{-1}	Lan	2	3	2	5	8	30	3
	GWL_{48}	cm	Both	-157	-142	-149	-135	-142	-121	-162
	Conditions	-	Both	dry	dry	dry	wet	wet	very wet	dry

3.2.2. Description of the flowing drainage network and stream chemistry changes during the 2021-09-29 event

In this section, we describe the hydrological and hydrochemical responses in the two catchments before and during the 16 mm rainfall event on 2021-09-29. We selected this event because it was the largest of the three events for which hydrograph separation was possible for both catchments. Moreover, most of the precipitation in the Erlenbach area has a low intensity, i.e., 10-min precipitation < 3 [mm h^{-1}] (van Meerveld et al., 2018). Therefore, we used the event on 2021-09-29 as an emblematic example of the flowing drainage network and stream chemistry dynamics during small events with dry antecedent conditions. Figure 4 provides a detailed insight into the spatiotemporal variations in the hydrometric response (i.e., changes in streamflow, groundwater levels, and f_{FDNL}) and streamwater chemistry, including the event water contributions. Similar figures for the other events can be found in the supplementary materials (Fig. S3-S8).

Before rainfall started (i.e., until time step t_1 in Fig. 4), streamwater chemistry at the outlets of Lan and Cha was typical of baseflow conditions during the study period (Fig. 2), i.e., the concentrations of weathering-derived solutes (e.g., calcium, silica, sulfate) were high and concentrations of nitrate, chloride, and iron were low (Fig. 3 and Fig. 4b). This is consistent with our expectation that groundwater is the main source of streamflow during baseflow conditions. The concentrations of chloride and

https://doi.org/10.5194/hess-2024-67
Preprint. Discussion started: 2 April 2024


Hydrology and Earth System Sciences
Discussions

iron were higher in Lan than Cha, likely due to local groundwater sources that are rich in these solutes (e.g., LGW3, Fig. 2, see section 3.1.1). The end member mixing analyses based on silica and δ^2H suggest that soil water did not contribute to baseflow.

The flowing drainage network in Lan was fragmented and short (f_{FDNL}=0.09). The streams were flowing close to the catchment outlet, as well as locally in the middle of the catchment (but note the network was disconnected, i.e., streamflow infiltrated into the subsurface further downstream; t_1 in Fig. 4a). In Cha, groundwater emerged from perennial springs in the central part of the catchment at the bottom of the steep hillslope (compare Fig. 1 and Fig. 4) and the continuous flow from this spring caused the specific discharge in Cha and f_{FDNL} (0.6 vs 0.09) to be higher than in Lan (Fig. 4e).

After the onset of rainfall, f_{FDNL} in Lan increased within approximately five hours from 0.09 to 0.42 (t_1-t_2 in Fig. 4) because more uphill channels started to flow. The drainage network did not expand to its full extent during this event, likely because the groundwater levels did not reach the more permeable rooting zone at around 0-20 cm depth, e.g., the water level in LGW1 rose from 42 to 23 cm below the soil surface. The event water fraction (f_e) increased within six hours to 0.34, i.e., for slightly longer than f_{FDNL}. Assuming an on average 0.2 m wide stream, the flow that could be generated from rainfall falling directly on the flowing stream network was larger than the observed increase in streamflow as well as the observed event water flux (due to the very small event water fraction at this time) when the intensity of rainfall was high (1:30-2:30) and shortly after, i.e., for approximately first two hours of the event (Fig. S13). This calculation suggests that at the start of the event rain falling on disconnected stream segments did not immediately make it to the outlet and that some water will have infiltrated into the channel. However, afterward, the event water flux was always larger than the discharge that could have been produced by the rain falling on the channel. Over the entire event, the total event water flux was more than six times the potential discharge of the rainfall falling on the channel. This suggests that other areas (e.g., saturated areas) must have contributed to event water to streamflow as well.

During the time of the rapid increase in streamflow and f_{FDNL} in Lan chloride and nitrate concentrations increased substantially until shortly after the peak flow and before peak f_{FDNL}, suggesting the mobilization from dry stream channels or the material that was stored in them. Interestingly, the f_{FDNL}, f_e, and the groundwater level remained high for more than ten hours after rainfall stopped, whereas discharge decreased from 34 [l min^{-1}] to 14 [l min^{-1}] (t_3 to t_4, Fig. 4b). Solute concentrations in streamflow remained roughly constant during this time as well.

In Cha, the flowing drainage network expanded rapidly from 0.60 to 0.84 in less than one hour after rainfall started (t_1 to t_3 in Fig. 4e). Contrary to Lan, f_{FDNL} in Cha returned to the pre-event conditions within 1.5 hours after the rainfall stopped. The contribution of event water in Cha increased as quickly as in Lan, but peak f_e was much smaller (< 15% at t_3), likely because the geomorphic drainage network in Cha was generally much shorter than in Lan (15.2 [km^{-1}] vs 40 [km^{-1}]). The groundwater

https://doi.org/10.5194/hess-2024-67
Preprint. Discussion started: 2 April 2024


Hydrology and Earth System Sciences
Discussions

levels in GBGW1 were still low at the time that peak flow occurred (at about 53 cm below the surface) but kept rising slowly afterward (to about 50 cm below the surface). Discharge and f_{FDNL} returned quickly to pre-event conditions (t_3 to t_4 in Fig. 4e). Similar to Lan, weathering-derived solutes in the Cha streamwater were diluted. Concentrations of iron and chloride increased, suggesting a connection to groundwater from other stores and interflow in topsoil. In contrast to Lan, nitrate concentrations in Cha streamwater decreased slightly during the event.

https://doi.org/10.5194/hess-2024-67
Preprint. Discussion started: 2 April 2024

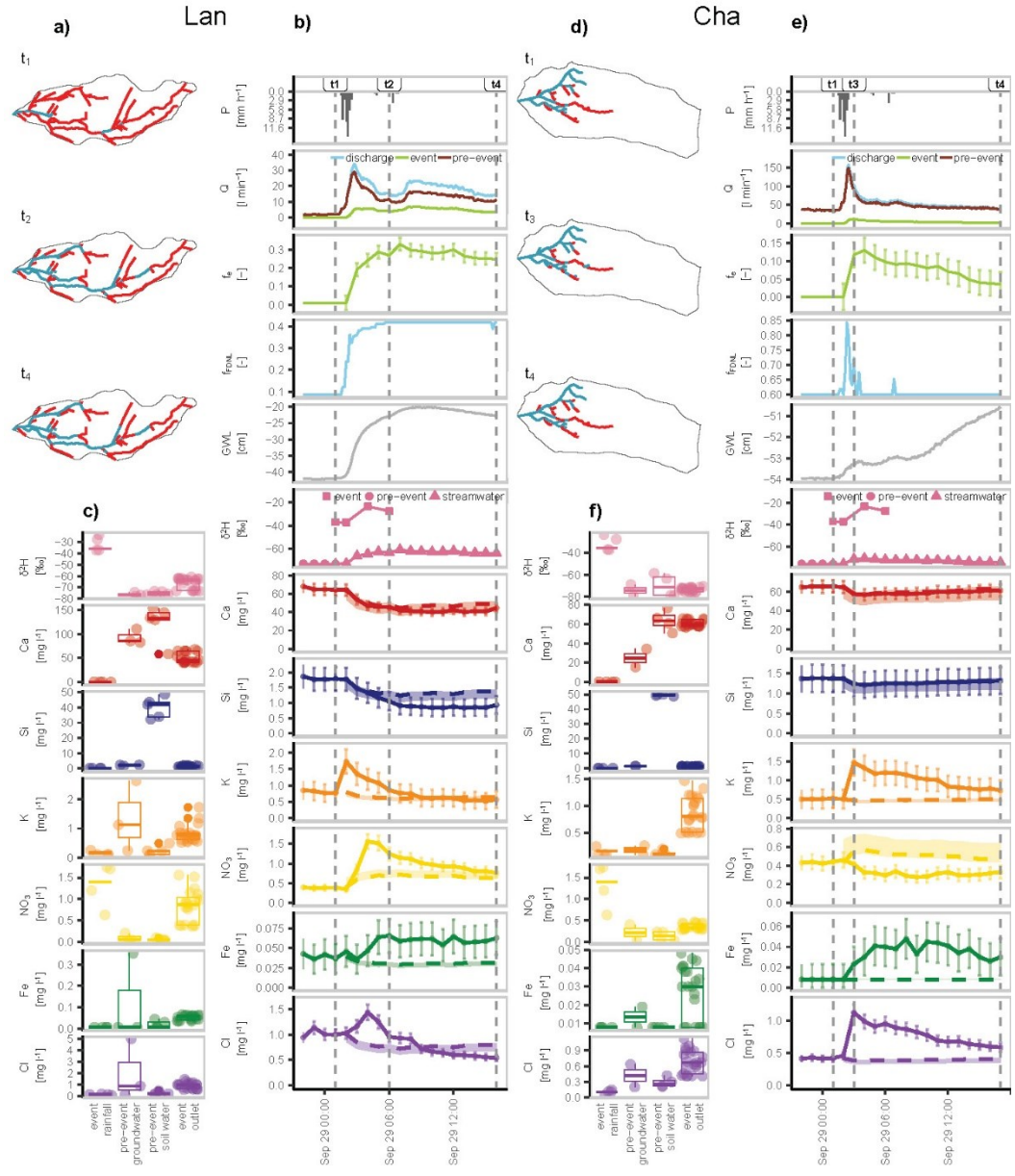

Figure 4: Maps of the flowing (blue) and not flowing (red) reaches of the channel network during three selected times during the 2021-09-29 event (a, d); time-series of hydrologic variables, δ^2H and solute concentrations, and the results of the hydrograph separation (b, c); box plots of the concentrations of the samples collected at the catchment outlet during the event, the weighted mean of the rainfall sampled during the event, pre-event groundwater samples, and pre-event soil water (lysimeter) samples (c, e) for the Lan (left) and Cha (right) catchments. In panels a, b, d and e, t_1 represents the start of the event, t_2, and t_3 mark the time of the maximum extension of the flowing drainage network (i.e. the largest f_{FDNL}), and t_4 marks the time when the last sample was collected during the event. Boxes in panels c and f show the 1st, 2nd, and 3rd quartiles and whiskers extend to the minimum and maximum values. GWL in panels b and e stands for groundwater level and shows data from locations LGW1 (Lan) and CBGW2 (Cha). The error bars in panels b and e represent the uncertainty of the laboratory measurements (solutes) or the calculated standard error (fe), the dashed line represents the expected concentration based on the hydrograph separation and the shaded areas the upper and lower bound of the expected concentrations based on the standard error of f_e. The data for the other six events are presented in the supplementary material (Figures S3-S8).

https://doi.org/10.5194/hess-2024-67
Preprint. Discussion started: 2 April 2024


Hydrology and Earth System Sciences
Discussions

3.3. Inferences about runoff generation mechanisms in the Lan catchment

3.3.1. Rainfall on wet channels and saturated areas

The event water fraction increased with the fraction of the flowing drainage network (Fig. 5a) and varied from 0 to 0.9 for the three events for which hydrograph separation was possible for the Lan catchment. Moreover, both f_{FDNL} and f_e were higher when streamflow increased more during the event (ΔQ; Table 1). During the first two hours of the events, event water fractions increased slowly (i.e., $f_e < 0.2$; Fig. 5a), but they increased more rapidly once f_{FDNL} was higher than 0.4 (Fig. 5a), which marks the transition from a fragmented to a connected drainage network (Bujak-Ozga et al., 2023). This suggests that the connection of the flowing drainage network leads to an increased contribution of event water at the catchment outlet. However, direct precipitation on the flowing stream channel was not sufficient to explain the calculated flux of event water (Fig. S13-S16). Furthermore, the event water fractions remained high after the rainfall stopped and discharge decreased (Fig.4, Fig.S3-S8). This suggests that the event water must have come from areas from areas outside the channel network, e.g., saturated overland flow and shallow (root zone) interflow. Saturated overland flow has been observed at many locations throughout the neighboring Studibach catchment, especially on the wet meadow areas (van Meerveld et al., 2019). Infiltration excess overland flow likely plays a minor role as the hydraulic conductivity of the soil at the surface was generally higher than the rainfall intensities (van Meerveld et al., 2019; Wadman 2023).

The increased concentrations of iron during rainfall events are likely caused by the transport of more soluble and mobile ferrous iron minerals from the reduced conditions of saturated areas (typical for Gleysoils; Hewitt et al., 2021) that become connected during rainfall events and start contributing to streamflow at the outlet. Iron concentrations increased sharply from circa 0.02 to 0.9 [mg l^{-1}] when f_{FDNL} increased to 0.5 and the network became connected (Fig. 5s). This increase was consistent for all events. When f_{FDNL} in Lan exceeds 0.5, surface flow occurs in multiple shallow channels and artificial ditches, highlighting the saturation of the system as well (Bujak-Ozga et al., 2023). Moreover, iron concentrations were the most variable at low discharge, and we observed a slight mobilization when the network became connected. When shallow channels and artificial ditches were flowing, iron concentrations were high, showed chemostatic behavior, and varied less (Fig. S12q). Previous research suggested that a decrease in the coefficient of variation in solute concentration with increasing discharge can be caused by higher connectivity due to the wetter conditions and spatial variations in solute concentrations within the catchment (Knapp et al., 2022). Thus, the high spatial heterogeneity in iron concentrations could contribute to the observed CQ relationship for iron in Lan. Indeed, we observed iron concentrations of around 0.7 [mg l^{-1}] in one of the groundwater wells in Lan (LGW1; Fig. 3), suggesting that locally higher iron concentrations are present in Lan, depending on the redox conditions. This is supported by previous studies in the Lan area (Hagedorn et al., 2001) and the neighboring Studibach catchment (Kiewiet et al., 2019) that found high iron concentrations in soil and groundwater in waterlogged depressions and riparian-like areas, and

https://doi.org/10.5194/hess-2024-67
Preprint. Discussion started: 2 April 2024


Hydrology and Earth System Sciences
Discussions

lower concentrations in aerobic mounds and hillslope groundwater. Similar results have also been found in other catchments. For example, research in over eighty German catchments showed that mean iron concentrations in streamwater were high in flatter catchments where shallow groundwater tables create conditions favorable for reductive processes (Tittel et al., 2022).

3.3.2. Groundwater flow

Pre-event water was the dominant source of streamwater at the Lan catchment outlet (Fig. 5a). The high pre-event water fractions (Fig. 5a) during the first two hours of the events suggest that the increase in discharge was mainly related to an increase in pre-event water (e.g., Fig. 4b, Fig. S3b-S8b). The considerable increase in pre-event water during the event suggests that the infiltrating rainfall causes additional groundwater to be released (cf. the low event water contributions as a fraction of precipitation observed by von Freyberg et al., 2018).

The increase in pre-event water at the catchment outlet is likely controlled by the rise of the groundwater levels into more permeable topsoil layers and the expansion of the groundwater contributing source area (cf. Rinderer et al, 2019). Previous research has suggested that vertical differences in weathering-derived solutes can cause dilution patterns as well (Botter et al., 2020; Knapp et al., 2022). In Lan, calcium concentrations in the shallow soils increase with depth below the surface (Hagedorn et al., 2001), similar to the neighboring Studibach catchment (Kiewiet et al., 2020; Bruppacher, 2022). This vertical stratification of weathering-derived solutes in the subsurface would lead to a decrease in concentrations as the groundwater levels rise into the shallower layers. However, this process likely plays a minor role in Lan because the good correspondence between the observed concentrations and those expected based on simple dilution with event water for weathering-derived solutes (calcium, sulfate, sodium, magnesium, silica) (e.g., Fig. 4) suggests that the concentrations of these solutes are mainly affected by the dilution of the groundwater with event water. Furthermore, the time of the groundwater response and dilution patterns did not coincide for many events (e.g., Fig. S7). Finally, the large spatial variation in groundwater chemistry may mask the effect of any vertical variation (Fig. 3).

3.3.3. Soil water and interflow

The high concentrations of silica and magnesium in soil water (i.e., samples from the lysimeters) were used to infer the importance of interflow in the subsoil (i.e., flow at ca. 30 cm from the soil surface). The dilution patterns for these solutes were similar to those of the weathering-derived solutes (e.g., Fig 4. and Fig. 5i,k). This suggests a very small contribution from soil water at the Lan catchment outlet, which is further supported by the EMMA results that indicated that f_{sw} was negligible. Similar results were found by Kiewiet et al. (2020) for the Studibach catchment, where pre-event groundwater was the dominant source of streamflow and soil water contributions were minimal for three out of the four analyzed events.

https://doi.org/10.5194/hess-2024-67
Preprint. Discussion started: 2 April 2024


Hydrology and Earth System Sciences
Discussions

We observed more pronounced clockwise hysteresis for potassium and chloride (Fig. 5m,o; Fig. S11a; Fig. S10g) than for the other solutes. The increase in potassium and chloride concentrations at the catchment outlet (i.e., above the expected concentration according to the simple mixing of baseflow and rainfall (Fig. 4b and Fig. S8b) means that some additional sources that are rich in those nutrients contributed to the streamflow. Relatively high potassium and chloride concentrations were assumed to be indicative of contributions from soil water in the Studibach in previous studies (Kiewiet et al, 2020). A study of vertical concentration profiles in soils in the Studibach catchment (Bruppacher, 2022) highlighted the high variation in potassium concentrations with depth below the surface and that the concentrations were the highest in the shallowest soil (12.5 cm below the surface). Thus, the observed hysteresis in potassium concentrations could, indeed, be caused by a contribution of water from the shallow topsoil (i.e., at ~ 0-15 cm below the surface, above the installed lysimeters). However, they could also have been caused by the rising groundwater levels and expansion of the groundwater contributing area because groundwater in Lan was highly variable in chloride and potassium concentrations (Fig. 3), which is typical for the Alptal catchments (Kiewiet et al. (2019); Knapp et al., 2020). Due to this high spatial variability (Fig. 3), additional measurements would be required to determine if the changes in chloride and potassium concentrations are caused by the contribution of shallow soil water and or different groundwater source areas.

Knapp et al. (2020) also reported similarity in potassium and chloride dynamics and predominantly mobilization of chloride during events for the Erlenbach catchment. They also reported a larger slope of the CQ relationship for large events during dry conditions, which agrees with the differences in the CQ relation observed for the 2021-09-16 and 2021-09-19 events (Fig. 5o). However, there were also differences in the response timing (e.g., Fig. 4b) and/or concentrations (e.g., Fig. S8b). Chloride concentrations were less variable at lower than at higher discharges (Fig. S12q). Unlike chloride, potassium concentrations are affected by biological processes, which could contribute to its general high variability (Fig.S12o), especially for the events with dry antecedent conditions (Fig. S10g; 2021-09-10).

3.3.4. Flush of nitrate from previously dry channels

Nitrate concentrations in streamwater increased more than expected from the mixing of event and pre-event water in Lan (Fig. 4b, Fig. S3b-S8b), suggesting a mobilization of nitrate during stream network expansion (Fig. 5q). The increase in nitrate concentrations occurred during all rainfall events but the magnitude of the change varied between events. For the smallest event during dry conditions on 2021-09-10 (Table 1), streamwater nitrate concentrations increased by only 0.3-0.8 [mg l^{-1}]. During this event, many channels remained dry, and f_{FDNL} (max f_{FDNL}: 0.4) and streamflow remained low (ΔQ: 16 [l s^{-1}]). There was especially a lack of response in the reaches with a low flow persistency. The largest event (2021-09-16), which occurred during moderately dry antecedent conditions, caused the expansion of the full network. For this event, nitrate concentrations were much higher and increased up to 3 [mg l^{-1}]. For the event on 2021-09-19, only three days later, with wet antecedent conditions, an almost full expansion of the FDNL (f_{FDNL}: 0.9), and the second highest peak discharge, nitrate concentrations

https://doi.org/10.5194/hess-2024-67
Preprint. Discussion started: 2 April 2024


Hydrology and Earth System Sciences
Discussions

remained below 1 [mg l^{-1}]. Such inter- and intra-event variability in nitrate concentrations is not surprising. The nitrate pool was likely already mobilized during the preceding event and there had not been enough time for a new nitrate pool to accumulate. The two other events that were also characterized by relatively high nitrate concentrations (2021-10-12 and 2021-10-21) occurred in October when the vegetation started shedding leaves and more detritus accumulated on the surface and in the dry channels. Nitrate "first flushes" following the reconnection of flow have been observed in other studies in intermittent streams as well (e.g., von Schiller et al., 2011; Merbt et al., 2016). Mineralization of organic matter from accumulated detritus and nitrification in the streambeds during the dry phase are a main source of inorganic nitrogen in streams (Baldwin et al., 2005, Woodward et al., 2015, Merbt et al., 2016; von Schiller et al., 2017; Arce et al., 2018). Moreover, Merbt et al. (2016) showed that ammonia oxidation in dry streambeds can contribute to roughly 50% of nitrate flush in intermittent streams. The drainage network in Lan has a large number of reaches that fall dry between rainfall events (i.e., that have a low flow persistency), allowing for nitrate accumulation in the dry streambeds.

Accumulation of nitrate can also occur in soils, but both groundwater and soil water in Lan were characterized by low nitrate concentrations (Fig. 2, Fig. 4c). Thus, groundwater and soil water are unlikely to contribute to higher nitrate concentrations at the catchment outlet. Kiewiet et al. (2019) showed that in the neighboring Studibach catchment, median nitrate concentrations in groundwater were also low (0.04 and 0.1 [mg l^{-1}] in catchment areas underlain by Schlieren and Ragazer Flysch, respectively). A lack of nitrate in deeper soil horizons is typical for gleysols (Hewitt et al., 2021) due to the high/perched groundwater tables and anaerobic conditions. In areas close to Lan, nitrate was present only in topsoil (0-10 cm depth), and even there only in relatively low concentrations (median concentrations < ~0.5 [mg l^{-1}]). In the deeper soil layers, nitrate concentrations were below the detection limit (Hagedorn et al., 2001).

Dry deposition can be a source of nitrate in forested catchments and could be the reason that a few rainfall samples taken at the beginning of the events with higher nitrate concentrations (Fig. S7, Fig. S8). Hagedorn et al. (2001) showed that concentrations in throughfall are also higher (median: ca. 2.4 [mg l^{-1}]) than for precipitation. Considering the high percentage of forest in Lan, throughfall could be a potential source of nitrate for Lan. However, nitrate concentrations at the Lan catchment outlet were highest when segments with low flow persistency were flowing (Fig. S12s), and nitrate concentrations remained high even after rainfall ended (Fig. 4b, t_3-t_4), therefore, a nitrate "flush" due to mobilization from the previously dry streambeds is a more likely cause for the observed nitrate dynamics at the catchment outlet.

3.3.5. Summary of dominant flow processes in Lan

To summarize, the connection of the previously fragmented drainage network plays an important role in the transport of rainfall and overland flow to the catchment outlet. The expansion of the drainage network also results in a flush of nitrate from previously dry channel beds (Fig. 6e). The role of interflow in the subsoil during rainfall events is likely minor, as most of the

https://doi.org/10.5194/hess-2024-67
Preprint. Discussion started: 2 April 2024


Hydrology and Earth System Sciences
Discussions

interflow occurs in the more permeable topsoil. Groundwater flow is the dominant source of streamflow at the catchment outlet, especially during the initial hours of rainfall events. Later in the events, other groundwater source areas connect and start to contribute to streamflow, especially during wetter conditions and larger events. During these wetter conditions, overland flow or lateral flow of event water through the topsoil becomes an important source of streamflow as well.

https://doi.org/10.5194/hess-2024-67
Preprint. Discussion started: 2 April 2024

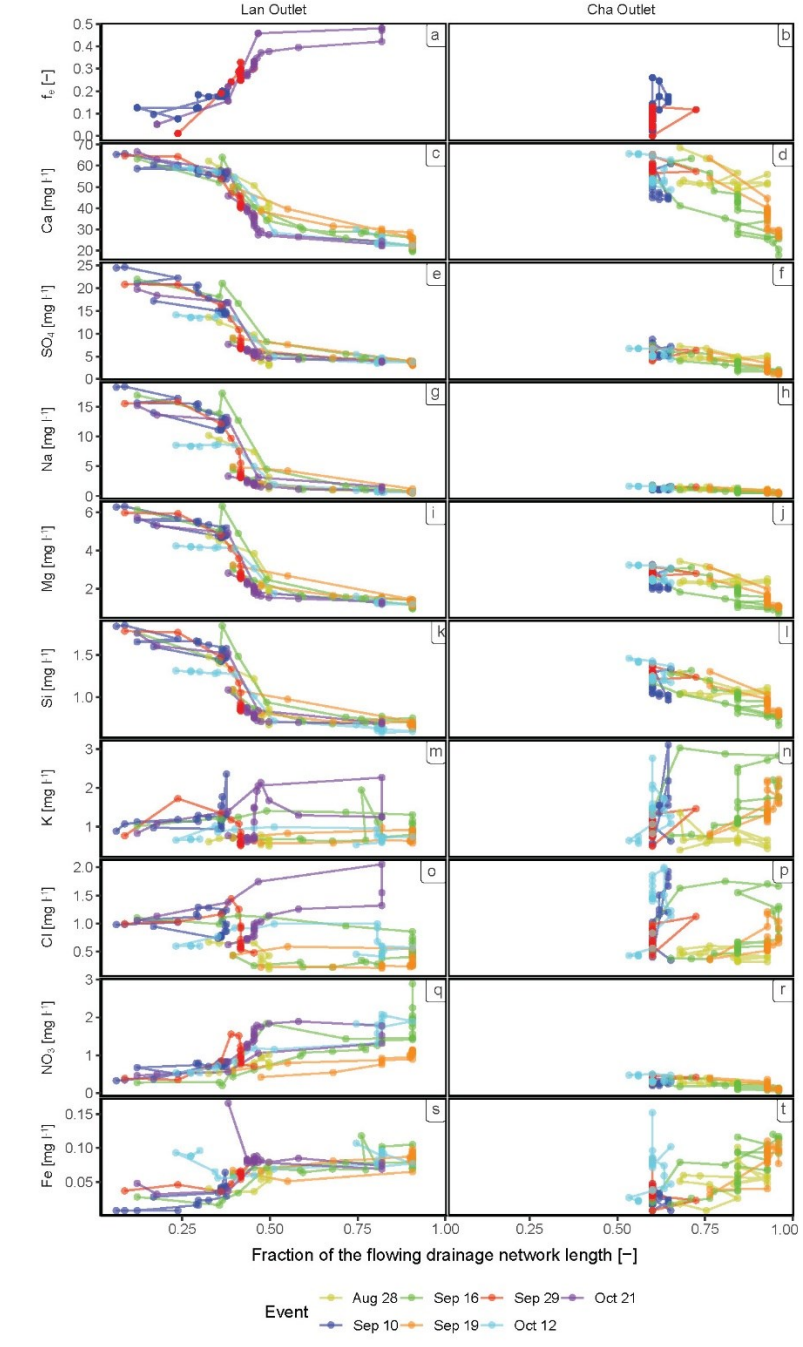

Figure 5: Event-water fractions (fe) and solute concentrations plotted as a function of the fraction of the drainage network that was flowing (f_{FDNL}) at the time that the sample was collected for the Lan catchment (left-hand panel) and the Cha catchment (right-hand panel). The different colors represent the different events. One chloride measurement (12-10-2021: 4.68 [mg l^{-1}]) and two potassium measurements (2021-09-11: 5.66 [mg l^{-1}], and 3.99 [mg l^{-1}]) from Lan are not shown to increase the visibility of the other data points. For the graphs showing the event-water fractions (f_e) and solute concentrations as a function of the discharge see Fig. S11, for the graphs showing the concentrations as a function of the event-water fractions, see Fig. S12.

https://doi.org/10.5194/hess-2024-67
Preprint. Discussion started: 2 April 2024


Hydrology and Earth System Sciences
Discussions

3.4. Inferences about runoff generation mechanisms in the Cha catchment

3.4.1. Rainfall on wet channels and saturated areas

The expansion and contraction of the flowing drainage network in Cha were more constrained than in Lan: f_{FDNL} changed only between 0.5 and 0.9 (Fig. 5). There was also no apparent rapid transition between a fragmented and connected network. The changes in event water fractions and solute concentrations were also different from those in Lan (Fig. S11 and Fig. S10). The event water fractions for the two events for which it could be calculated suggest that for small rainfall events event water played only a minor role in streamflow generation in Cha. Unlike Lan, event water fractions were not well related to the fraction of the flowing drainage network (Fig. 5b). The correlation of the event water fractions with the discharge was also poorer than for Lan (Fig. S12b).

Saturated overland flow is probably important in Cha as well. The CQ relation for iron, for example, showed chemodynamic behavior for the small events, and mobilization for the bigger events with the largest increases in streamflow (Fig. 5t, Table1). Increasing iron concentrations and decreasing nitrate concentrations in streamflow could suggest an increased input of water from the saturated area. The drainage network in Cha is located in the western, flatter part of the catchment. This part of the catchment is characterized by a wet area with shallow water tables, that are typical for Gleysols (Hewitt et al., 2021). The high groundwater levels and anoxic conditions are favorable for nitrate removal and can explain the higher iron and lower nitrate concentrations in soil and groundwater in this part of the catchment (CBGW1 and CBGW1LYS; Fig. 2) than the steeper eastern part of the catchment (CBGW2 and CBGW2LYS; Fig. 2), where there is probably more infiltration into the better drained drier soils and nitrate removal due to the vegetation uptake. Iron concentrations started to increase ca. two hours earlier in Cha than in Lan, but the streamflow response was generally faster for Cha than Lan as well. The faster response in Cha can simply be related to the spatial distribution of the source area within catchments (Knapp et al., 2022), or the steeper slope of the catchment.

3.4.2. Groundwater flow

The pre-event water fractions in Cha were higher than in Lan. Sulfate, magnesium, and sodium concentrations in baseflow were relatively low, suggesting that the groundwater that feeds the perennial springs is not very old. Calcium dissolves quickly, thus, concentrations in baseflow were comparable to Lan.

Similar to Lan, the observed variations in the concentrations of weathering-derived solutes (Ca, Na, SO_4, S, Mg, Si) for the two relatively small events matched the expected concentrations based on simple mixing of pre-event water and event water.

https://doi.org/10.5194/hess-2024-67
Preprint. Discussion started: 2 April 2024

635 However, for larger events, hysteresis occurs for calcium, magnesium, and silica. Moreover, the variability of weathering-derived solutes in Cha was higher at higher discharges (Fig. S12). In Lan, dilution is the dominant process that affects the concentrations of these solutes, but in Cha, there is an additional effect of the connection of the upper hillslope, which likely introduces variability in the measured concentrations at the outlet (as also indicated by the variability of the concentrations of groundwater, lysimeter, and baseflow samples taken across the catchment (Fig. 3). We, furthermore, observe more inter-event
640 variability in calcium concentrations than for sulfate and sodium in Cha. For the biggest event (2021-09-16), counter-clockwise hysteresis could be observed. Since shallow groundwater in Cha is depleted in calcium, such patterns might be indicative of shallower flowpaths. This is further supported by a small hysteresis in silica and magnesium concentrations during events (Fig. 5j,l).

645 **3.4.3. Soil water and interflow**

Similarly to Lan, concentrations of silica and magnesium in soil water in Cha showed a dilution pattern (e.g., Fig. 5j,l). The generally small contribution from soil water at the Cha catchment outlet was further supported by the results of the EMMA analysis for the two smaller events (calculated contributions from soil water 0%). Also, similar to Lan, chloride, and potassium showed a mobilization pattern (Fig. S12p,r) and increased more than could be expected based on simple mixing of rainfall and
650 baseflow (Fig. 4e and Fig. S8e). Moreover, chloride and potassium concentrations in Cha showed very similar clockwise hysteresis during rainfall events, which was more pronounced than for Lan (Fig. 5n,p; Fig. S11b; Fig. S10h). This could suggest that the same processes, i.e., interflow in the topsoil or a connection of groundwater sources with high chloride and potassium concentrations are responsible for the chloride and potassium dynamics in both catchments. After f_{FDNL} and f_e reached their maximum, potassium, and chloride generally decreased and returned to their expected values or were slightly
655 lower. These decreases tended to be faster for Lan than in Cha.

3.4.4. No nitrate flush

Interestingly, the nitrate response in Cha was very different from that observed in Lan. This suggests that the so-called nitrate "first flush" effect plays a minor role in Cha. Instead, nitrate concentrations were lower than expected from a simple mixing
660 of event and pre-event water (Fig. 4e). Nitrate concentrations in Cha did not exceed 1 [mg l^{-1}], while in Lan, concentrations during events went up to ca. 3 [mg l^{-1}] (Fig. 5-7). This is surprising, as one could expect the concentrations of nitrate to be slightly higher in Cha than in Lan because of the additional inputs from grazing cattle and less nutrient uptake by vegetation. Instead, nitrate concentrations in soil and groundwater were low for both Cha and Lan (Fig. 2-3). The difference in nitrate dynamics between Lan and Cha is likely related to the difference in the length of the channels that are dry for considerable
665 periods (i.e., segments with low flow persistency). In Cha, there are fewer channels in which nitrate could accumulate and subsequently be flushed out. Furthermore, there are fewer channels where direct precipitation, which is relatively high in

https://doi.org/10.5194/hess-2024-67
Preprint. Discussion started: 2 April 2024

nitrate (Fig. 3) can directly contribute to runoff. Instead, as discussed above, there is dilution of nitrate due to the contribution of runoff from saturated areas that are low in nitrate.

3.4.5. Summary of dominant flow processes in Cha

To summarize, in Cha the expansion of the flowing drainage network is limited, and the connection of the previously fragmented drainage network has a limited effect on stream water chemistry at the catchment outlet. Contrary to Lan, there is no nitrate flush, but instead a dilution due to the contribution of runoff from saturated areas (Fig. 6e). Groundwater flow is the dominant source of streamflow at the catchment outlet but during larger events and wetter conditions riparian-like groundwater areas connect and start contributing to streamflow as well. Interflow in the soil or shallow groundwater flow may play a more important role during large events as well.

https://doi.org/10.5194/hess-2024-67
Preprint. Discussion started: 2 April 2024

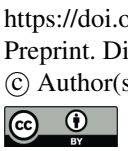

Hydrology and Earth System Sciences
Discussions

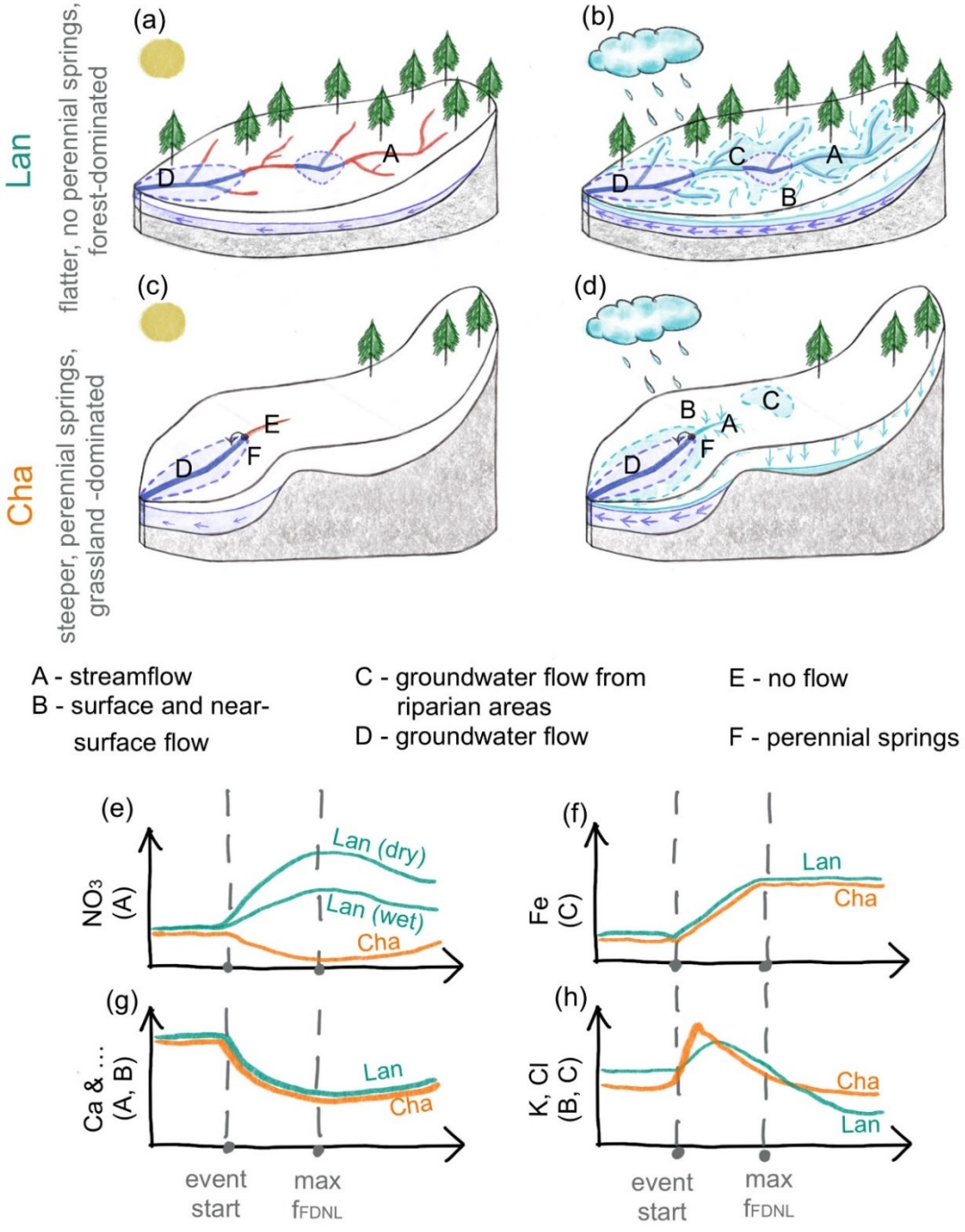

Figure 6: Conceptual diagram showing the flowing drainage network in Lan and Cha and the main processes leading to streamflow during baseflow conditions (a, c) and rainfall events (b, d). The related temporal variations in solute concentrations at the catchment outlet are shown for nitrate (e), iron (f), calcium and other weathering-derived solutes (g), and potassium and chloride (h). The green line represents the dynamics for Lan and the orange line for Cha. Two green lines for nitrate dynamics (e) represent the different magnitude of response in Lan during dry ("first flush") and wet antecedent conditions.

https://doi.org/10.5194/hess-2024-67
Preprint. Discussion started: 2 April 2024


Hydrology and Earth System Sciences
Discussions

4. Conclusions

In this study, we investigated how solute concentrations, event water fractions, and the flowing drainage network change during rainfall events in two small headwater catchments of similar size and soil and bedrock settings. In both catchments, groundwater was the main source of streamflow and the dynamics of the concentrations of the weathering-derived solutes could be explained by the mixing of event water and pre-event water (Fig. 8). The event water contribution at the beginning of rainfall events could be explained by rain falling on the channels. For wetter conditions, overland flow from saturated areas (Fig. 8) or quick interflow from topsoil must have contributed event water to the stream as well. The contribution from the deeper (~30 cm) subsoil was relatively limited but the dynamics of the potassium and chloride concentrations suggest a contribution from interflow from the topsoil as well. There were also distinct differences in the hydrological and hydrochemical responses of the two catchments. In the flatter Lan catchment, the flowing drainage network expanded rapidly and up to 10-fold during rainfall events. The longer drainage network facilitated the contribution of direct runoff and caused the mobilization of nitrate from channel reaches that were previously dry. In the steeper Cha catchment with a more stable flowing drainage network, nitrate was diluted during events due to the contribution of runoff from saturated areas (Fig. 8). However, the solute dynamics in Lan and Cha during rainfall events were similar to the ones previously described for the larger Erlenbach catchment (Knapp et al., 2020), which could help to upscale the observed processes to larger areas in the future. Overall, this study highlights the high variability in the flowing stream network and stream chemical responses for neighboring catchments and how information on the flowing stream network can help to understand stream chemistry dynamics and interpret runoff processes.

Data availability

Hydrometric data from this study is available on EnviDat (Bujak-Ozga et al., 2023b). We are in the process of uploading the hydrochemistry data to EnviDat.ch, where most of the data from the Alptal catchments are stored.

Author contribution

IBO, IvM and JvF conceptualized the study; IBO collected, cured and visualized the data; IBO analyzed and interpreted the data with support from all co-authors; IBO wrote the manuscript draft; IvM, JvF, MZ, AR and PB reviewed and edited the manuscript. IvM, JvF, and AR supervised the project.

https://doi.org/10.5194/hess-2024-67
Preprint. Discussion started: 2 April 2024

Competing interests

The authors declare that they have no conflict of interest. Some authors are members of the editorial board of journal PNAS.

Acknowledgements

We sincerely thank Marius Luder and Nina Nagel for their help in equipment installation and maintenance, sample collection and preparation and data processing. We thank Barbara Strobl, Joshua Haas, Alex Karapanscev, Rick Assendelft, Florian Käslin, Pascal Arpagaus, Florian Lustenberger, Kari Steiner, and Stefan Boss for helping with fieldwork in the Alptal catchment. This work was funded by the Swiss National Science Foundation grant (PR00P2_185931) awarded to JvF.

This draft manuscript is distributed solely for purposes of scientific peer review. Its content is deliberative and pre-decisional, so it must not be disclosed or released by reviewers. Because the manuscript has not yet been approved for publication by the U.S. Geological Survey (USGS), it does not represent any official USGS finding or policy.

References

Acuña, V., Datry, T., Marshall, J., Barceló, D., Dahm, C. N., Ginebreda, A., ... & Palmer, M. A. (2014). Why should we care about temporary waterways? Science, 343(6175), 1080-1081.

Addy, K., Gold, A. J., Welsh, M. K., August, P. V., Stolt, M. H., Arango, C. P., & Groffman, P. M. (2019). Connectivity and nitrate uptake potential of intermittent streams in the Northeast USA. Frontiers in Ecology and Evolution, 7, 225.

Arce, M. I., Von Schiller, D., Bengtsson, M. M., Hinze, C., Jung, H., Alves, R. J. E., ... & Singer, G. (2018). Drying and rainfall shape the structure and functioning of nitrifying microbial communities in riverbed sediments. Frontiers in microbiology, 9, 2794.

Arce, M. I., Mendoza-Lera, C., Almagro, M., Catalán, N., Romaní, A. M., Martí, E., ... & Von Schiller, D. (2019). A conceptual framework for understanding the biogeochemistry of dry riverbeds through the lens of soil science. Earth-Science Reviews, 188, 441-453.

Assendelft, R. S., & van Meerveld, H. I. (2019). A low-cost, multi-sensor system to monitor temporary stream dynamics in mountainous head- water catchments. Sensors, 19(21), 4645.

Baldwin, D. S., Rees, G. N., Mitchell, A. M., & Watson, G. (2005). Spatial and temporal variability of nitrogen dynamics in an upland stream before and after a drought. Marine and Freshwater Research, 56(4), 457-464.

Botter, G., & Durighetto, N. (2020). The stream length duration curve: A tool for characterizing the time variability of the flowing stream length. Water Resources Research, 56(8), e2020WR027282.

Botter, M., Li, L., Hartmann, J., Burlando, P., & Fatichi, S. (2020). Depth of solute generation is a dominant control on concentration-discharge relations. Water Resources Research, 56(8), 2019WR026695. https://doi.org/10.1029/2019WR026695

Botter, G., Vingiani, F., Senatore, A., Jensen, C., Weiler, M., McGuire, K., ... & Durighetto, N. (2021). Hierarchical climate-driven dynamics of the active channel length in temporary streams. Scientific reports, 11(1), 21503.

Bruppacher, A. (2022). Spatial and temporal changes in soil water and groundwater chemistry in the Studibach catchment. Master's Thesis. University of Zurich.

Bujak-Ozga, I. (2023). TempAqua App iOS for Intermittent Streams Mapping (v2.3.1). Zenodo. https://doi.org/10.5281/zenodo.10035289

Bujak-Ozga, I., van Meerveld, H. J., Rinaldo, A., & von Freyberg, J. (2023). Short-term dynamics of drainage density based on a combination of channel flow state surveys and water level measurements. Hydrological Processes, 37(12), e15041.

Bujak-Ozga, I., van Meerveld, I., Rinaldo, A., & von Freyberg, J. (2023b). Short-term drainage density dynamics dataset. EnviDat. https://doi.org/10.16904/envidat.450

Burrows, R. M., Rutlidge, H., Bond, N. R., Eberhard, S. M., Auhl, A., Andersen, M. S., ... & Kennard, M. J. (2017). High rates of organic carbon processing in the hyporheic zone of intermittent streams. Scientific Reports, 7(1), 13198.

Christophersen, N., & Hooper, R. P. (1992). Multivariate analysis of stream water chemical data: The use of principal components analysis for the end-member mixing problem. Water Resources Research, 28(1), 99-107.

Covino, T. (2017). Hydrologic connectivity as a framework for understanding biogeochemical flux through watersheds and along fluvial networks. Geomorphology, 277, 133-144.

https://doi.org/10.5194/hess-2024-67
Preprint. Discussion started: 2 April 2024

Datry, T., Boulton, A. J., Fritz, K., Stubbington, R., Cid, N., Crabot, J., & Tockner, K. (2023). Non-perennial segments in river networks. Nature Reviews Earth & Environment, 1-16.

Dodds, W. K., Gido, K., Whiles, M. R., Fritz, K. M., & Matthews, W. J. (2004). Life on the edge: The ecology of Great Plains prairie streams. Bioscience, 54(3), 205–216.

Durighetto, N., Vingiani, F., Bertassello, L. E., Camporese, M., & Botter, G. (2020). Intraseasonal drainage network dynamics in a headwater catchment of the Italian Alps. Water Resources Research, 56(4), e2019WR025563.

Durighetto, N., & Botter, G. (2021). Time-lapse visualization of spatial and temporal patterns of stream network dynamics. Hydrological Processes, 35(2).

Durighetto, N., & Botter, G. (2022). On the relation between active network length and catchment discharge. Geophysical Research Letters, 49(14), e2022GL099500.

Durighetto, N., Mariotto, V., Zanetti, F., McGuire, K. J., Mendicino, G., Senatore, A., & Botter, G. (2022). Probabilistic description of streamflow and active length regimes in rivers. Water Resources Research, 58(4), e2021WR031344.

Fischer, B. M. C., Rinderer, M., Schneider, P., Ewen, T., and Seibert, J.: Contributing sources to baseflow in pre-alpine headwaters using spatial snapshot sampling, Hydrol. Process., 29, 5321-5336, 10.1002/hyp.10529, 2015.

Fovet, O., Belemtougri, A., Boithias, L., Braud, I., Charlier, J. B., Cottet, M., ... & Datry, T. (2021). Intermittent rivers and ephemeral streams: Perspectives for critical zone science and research on socio-ecosystems. Wiley Interdisciplinary Reviews: Water, 8(4), e1523.

Gal, J. Y., Bollinger, J. C., Tolosa, H., & Gache, N. (1996). Calcium carbonate solubility: a reappraisal of scale formation and inhibition. Talanta, 43(9), 1497-1509.

Genereux, D. (1998). Quantifying uncertainty in tracer-based hydrograph separations. Water Resources Research, 34(4), 915-919.

Giezendanner, J., Benettin, P., Durighetto, N., Botter, G., & Rinaldo, A. (2021). A note on the role of seasonal expansions and contractions of the flowing fluvial network on metapopulation persistence. Water Resources Research, 57(11), e2021WR029813.

Godsey, S. E., & Kirchner, J. W. (2014). Dynamic, discontinuous stream networks: Hydrologically driven variations in active drainage density, flowing channels and stream order. Hydrological Processes, 28(23), 5791-5803.

Gregory, K. J., & Walling, D. E. (1968). The variation of drainage density within a catchment. Hydrological Sciences Journal, 13(2), 61-68.

Hagedorn, F., Bucher, J. B., & Schleppi, P. (2001). Contrasting dynamics of dissolved inorganic and organic nitrogen in soil and surface waters of forested catchments with Gleysols. Geoderma, 100(1-2), 173-192.

Hale, R. L., & Godsey, S. E. (2019). Dynamic stream network intermittence explains emergent dissolved organic carbon chemostasis in headwaters. Hydrological Processes, 33(13), 1926-1936.

Hantke, R., Trümpy, R., BAumeler, A., Bollinger, D., Felber, P., Letsch, D., & Grünig, A. (2022). Blatt 1152 Ibergeregg—Geologischer Atlas der Schweiz 1: 25 000, Karte 175.

Hewitt, A.E., Balks, M.R., Lowe, D.J. (2021). Gley Soils. In: The Soils of Aotearoa New Zealand. World Soils Book Series. Springer, Cham. https://doi.org/10.1007/978-3-030-64763-6_5

Jaeger, K. L., & Olden, J. D. (2012). Electrical resistance sensor arrays as a means to quantify longitudinal connectivity of rivers. River Research and Applications, 28(10), 1843-1852.

Jaeger, K. L., Olden, J. D., & Pelland, N. A. (2014). Climate change poised to threaten hydrologic connectivity and endemic fishes in dryland streams. Proceedings of the National Academy of Sciences, 111(38), 13894-13899.

Jensen, C. K., McGuire, K. J., McLaughlin, D. L., & Scott, D. T. (2019). Quantifying spatiotemporal variation in headwater stream length using flow intermittency sensors. Environmental Monitoring and Assessment, 191, 226. https://doi.org/10.1007/s10661-019-7373-8

Kaplan, N. H., Sohrt, E., Blume, T., & Weiler, M. (2019). Monitoring ephem- eral, intermittent and perennial streamflow: A dataset from 182 sites in the Attert catchment, Luxembourg. Earth System Science Data, 11(3), 1363–1374.

Keller, P. S., Catalan, N., von Schiller, D., Grossart, H. P., Koschorreck, M., Obrador, B., ... & Marcé, R. (2020). Global CO2 emissions from dry inland waters share common drivers across ecosystems. Nature communications, 11(1), 2126.

https://doi.org/10.5194/hess-2024-67
Preprint. Discussion started: 2 April 2024

Kiewiet, L., von Freyberg, J., & van Meerveld, H. J. (2019). Spatiotemporal variability in hydrochemistry of shallow groundwater in a small pre-alpine catchment: The importance of landscape elements. Hydrological Processes, 33(19), 2502-2522.

Kiewiet, L., Van Meerveld, I., Stähli, M., & Seibert, J. (2020). Do stream water solute concentrations reflect when connectivity occurs in a small, pre-Alpine headwater catchment?. Hydrology and Earth System Sciences, 24(7), 3381-3398.

Knapp, J. L., Li, L., & Musolff, A. (2022). Hydrologic connectivity and source heterogeneity control concentration–discharge relationships. Hydrological Processes, 36(9), e14683.

Kulin, G., & Compton, P. R. (1975). A guide to methods and standards for the measurement of water flow (Vol. 13). US Department of Commerce, National Bureau of Standards.

Lamberti, G. A., Entrekin, S. A., Griffiths, N. A., & Tiegs, S. D. (2017). Coarse particulate organic matter: storage, transport, and retention. In Methods in stream ecology (pp. 55-69). Academic Press.

Merbt, S. N., Proia, L., Prosser, J. I., Martí, E., Casamayor, E. O., & Von Schiller, D. (2016). Stream drying drives microbial ammonia oxidation and first-flush nitrate export. Ecology, 97(9), 2192-2198.

Mari, L., Casagrandi, R., Bertuzzo, E., Rinaldo, A., & Gatto, M. (2014). Metapopulation persistence and species spread in river networks. Ecology letters, 17(4), 426-434.

Messager, M. L., Lehner, B., Cockburn, C., Lamouroux, N., Pella, H., Snelder, T., ... & Datry, T. (2021). Global prevalence of non-perennial rivers and streams. Nature, 594(7863), 391-397.

Meyer, J. L., Strayer, D. L., Wallace, J. B., Eggert, S. L., Helfman, G. S., Leonard, N. E.. The contribution of headwater streams to biodiversity in river networks 1., (2007), JAWRA Journal of the American Water Resources Association, 43(1), 86-103.

Mimeau, L., Künne, A., Branger, F., Kralisch, S., Devers, A., & Vidal, J. P. (2024). Flow intermittence prediction using a hybrid hydrological modelling approach: influence of observed intermittence data on the training of a random forest model. Hydrology and Earth System Sciences, 28(4), 851-871.

https://doi.org/10.5194/hess-2024-67
Preprint. Discussion started: 2 April 2024

Neal, C., & Kirchner, J. W. (2000). Sodium and chloride levels in rainfall, mist, streamwater and groundwater at the Plynlimon catchments, mid-Wales: inferences on hydrological and chemical controls. Hydrology and Earth System Sciences, 4(2), 295-310.

Peck, A. J., & Hurle, D. (1973). Chloride balance of some farmed and forested catchments in southwestern Australia. Water Resources Research, 9(3), 648-657.

Price, A. N., Jones, C. N., Hammond, J. C., Zimmer, M. A., & Zipper, S. C. (2021). The drying regimes of non-perennial rivers and streams. Geophysical Research Letters, 48(14), e2021GL093298.

Rinaldo, A., Gatto, M., Rodriguez-Iturbe, I. River networks as ecological corridors: A coherent ecohydrological perspective., 2018, Advances in Water Resources, 112, 27-58.

Rinderer, M., Van Meerveld, H. J., & Seibert, J. (2014). Topographic controls on shallow groundwater levels in a steep, prealpine catchment: When are the TWI assumptions valid?. Water Resources Research, 50(7), 6067-6080.

Rinderer, M., Van Meerveld, H. J., & McGlynn, B. L. (2019). From points to patterns: using groundwater time series clustering to investigate subsurface hydrological connectivity and runoff source area dynamics. Water Resources Research, 55(7), 5784-5806.

Schleppi, P., Muller, N., Feyen, H., Papritz, A., Bucher, J. B., and Fluehler, H.: Nitrogen budgets of two small experimental forested catchments at Alptal, Switzerland, Forest Ecol Manag, 101, 177-185, 10.1016/S0378-1127(97)00134-5, 1998.

Shumilova, O., Zak, D., Datry, T., von Schiller, D., Corti, R., Foulquier, A., ... & Zarfl, C. (2019). Simulating rewetting events in intermittent rivers and ephemeral streams: A global analysis of leached nutrients and organic matter. Global change biology, 25(5), 1591-1611.

Stähli, M. (2018). Longterm hydrological observatory Alptal (central Switzerland). EnviDat. https://www.doi.org/10.16904/envidat.380.

Stähli, M., Seibert, J., Kirchner, J. W., von Freyberg, J., & van Meerveld, I. (2021). Hydrological trends and the evolution of catchment research in the Alptal valley, central Switzerland. Hydrological Processes, 35(4), e14113.

https://doi.org/10.5194/hess-2024-67
Preprint. Discussion started: 2 April 2024

Stubbington, R., England, J., Wood, P. J., & Sefton, C. E. (2017). Temporary streams in temperate zones: recognizing, monitoring and restoring transitional aquatic-terrestrial ecosystems. Wiley Interdisciplinary Reviews: Water, 4(4), e1223.

Thoms, M. C. (2003). Floodplain–river ecosystems: lateral connections and the implications of human interference. Geomorphology, 56(3-4), 335-349.

Thoms, M. C., Southwell, M., & McGinness, H. M. (2005). Floodplain–river ecosystems: Fragmentation and water resources development. Geomorphology, 71(1-2), 126-138.

Tittel, J., Büttner, O., Friese, K., Lechtenfeld, O. J., Schuth, S., von Tümpling, W., & Musolff, A. (2022). Iron exports from catchments are constrained by redox status and topography. Global Biogeochemical Cycles, 36(1), e2021GB007056.

van Meerveld, H J; Fischer, Benjamin M C; Rinderer, Michael; Stähli, Manfred; Seibert, Jan (2018). Runoff generation in a pre-alpine catchment: A discussion between a tracer and a shallow groundwater hydrologist. Cuadernos de Investigacion Geografica, 44(2):429-452.

van Meerveld, H. J., Kirchner, J. W., Vis, M. J., Assendelft, R. S., & Seibert, J. (2019). Expansion and contraction of the flowing stream network alter hillslope flowpath lengths and the shape of the travel time distribution. Hydrology and Earth System Sciences, 23(11), 4825-4834.

von Freyberg, J., Studer, B., Rinderer, M., & Kirchner, J. W. (2018). Studying catchment storm response using event-and pre-event-water volumes as fractions of precipitation rather than discharge. Hydrology and Earth System Sciences, 22(11), 5847-5865.

von Schiller, D., Acuña, V., Graeber, D., Martí, E., Ribot, M., Sabater, S., ... & Tockner, K. (2011). Contraction, fragmentation and expansion dynamics determine nutrient availability in a Mediterranean forest stream. Aquatic Sciences, 73, 485-497.

von Schiller, D. V., Marcé, R., Obrador, B., Gómez-Gener, L., Casas-Ruiz, J. P., Acuña, V., & Koschorreck, M. (2014). Carbon dioxide emissions from dry watercourses. Inland waters, 4(4), 377-382.

von Schiller, D., Bernal, S., Dahm, C. N., & Martí, E. (2017). Nutrient and organic matter dynamics in intermittent rivers and ephemeral streams. In Intermittent rivers and ephemeral streams (pp. 135-160). Academic Press.

Wadman, M. (2023). Spatial variability of infiltration in a pre-alpine catchment. M.Sc. thesis. Wageningen University.

945

Walker, J. F., Hunt, R. J., Bullen, T. D., Krabbenhoft, D. P., & Kendall, C. (2003). Variability of isotope and major ion chemistry in the Allequash Basin, Wisconsin. Groundwater, 41(7), 883-894.

Ward, A. S., Schmadel, N. M., & Wondzell, S. M. (2018). Simulation of dynamic expansion, contraction, and connectivity in
950 a mountain stream network. Advances in Water Resources, 114, 64-82.

Ward, A. S., Wondzell, S. M., Schmadel, N. M., & Herzog, S. P. (2020). Climate change causes river network contraction and disconnection in the HJ Andrews Experimental Forest, Oregon, USA. Frontiers in Water, 2, 7.

955 Warix, S. R., Godsey, S. E., Lohse, K. A., & Hale, R. L. (2021). Influence of groundwater and topography on stream drying in semi-arid headwater streams. Hydrological Processes, 35(5), e14185.

Woodward, K. B., Fellows, C. S., Mitrovic, S. M., & Sheldon, F. (2015). Patterns and bioavailability of soil nutrients and carbon across a gradient of inundation frequencies in a lowland river channel, Murray–Darling Basin, Australia. Agriculture,
960 Ecosystems & Environment, 205, 1-8.

Zanetti, F., Durighetto, N., Vingiani, F., & Botter, G. (2022). Analyzing river network dynamics and the active length–discharge relationship using water presence sensors. Hydrology and Earth System Sciences, 26(13), 3497–3516.

965 Zimmer, M. A., Bailey, S. W., McGuire, K. J., & Bullen, T. D. (2013). Fine scale variations of surface water chemistry in an ephemeral to perennial drainage network. Hydrological Processes, 27(24), 3438-3451.

Zimmer, M. A., and McGlynn, B. L. (2018). Lateral, Vertical, and Longitudinal Source Area Connectivity Drive Runoff and Carbon Export Across Watershed Scales, Water Resour. Res., 54, 1576-1598, doi:10.1002/2017WR021718.

970

Zimmer, M. A., Burgin, A. J., Kaiser, K., & Hosen, J. (2022). The unknown biogeochemical impacts of drying rivers and streams. nature communications, 13(1), 7213.